Stockholm University

Bachelor Thesis

Degree Project in Marine Geology 30 hp

Sea floor characteristics of Asköfjärden and Fifångsdjupet, Trosa archipelago: deposition, erosion, and gas

Kay Hjälm

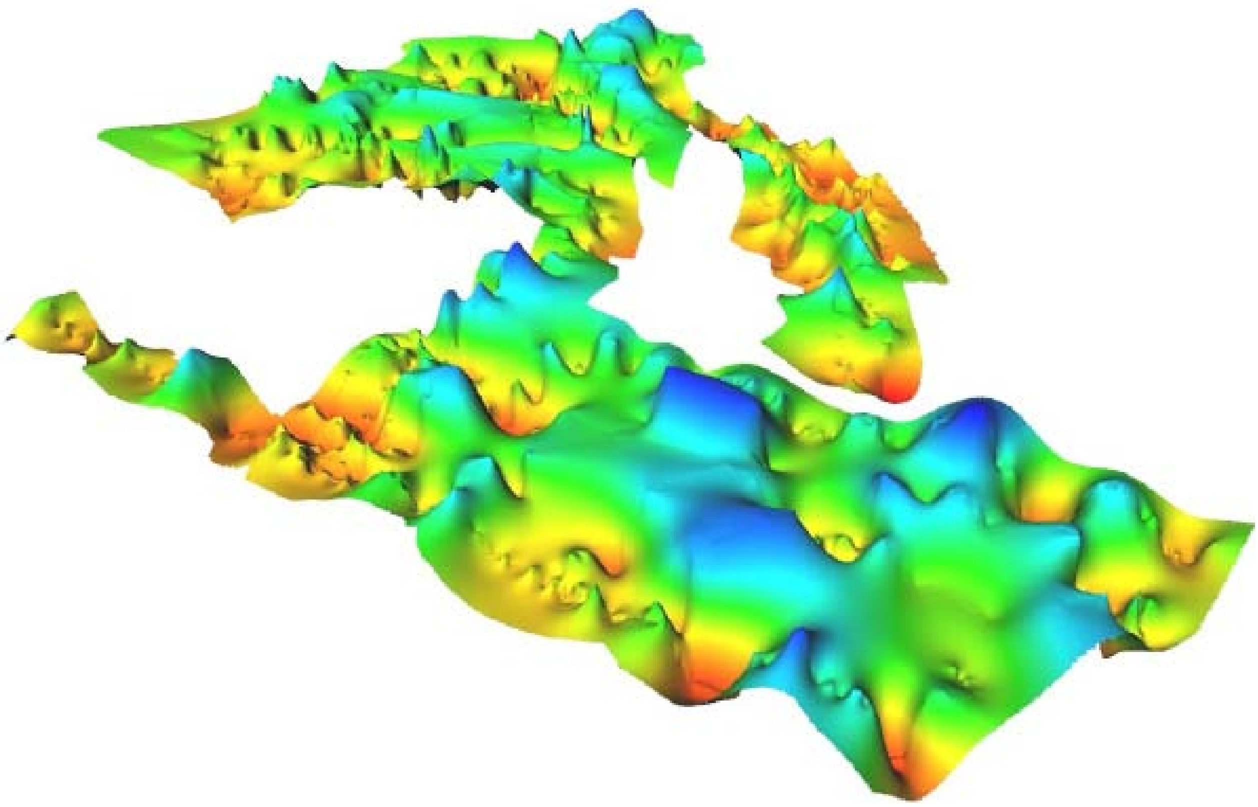

Stockholm 2013

Department of Geological Sciences
Stockholm University
SE-106 91 Stockholm

Abstract

The sea floor characteristics of Asköfjärden and Fifångsdjupet have been investigated using seismo-acoustic and core-sample data. Through interpretation three different postglacial events was distinguished which each represent a stage in the evolution of the Baltic. Closer study of one specific seismo-acoustic unit shows possible relations with the effects from deglaciation at the end of the Younger Dryas cold period. The area was just about covered by ice at the glacial maximum of this period of climatic setback, making it a part of the stagnation zone belt which is referred to as the Middle Swedish ice marginal zone. This period is possibly also reflected in the bathymetry of the area as it is interpreted from the constructed bathymetric grids. The constructed grids also give evidence of ongoing erosion at approximately 30-40 m in the northern parts of Asköfjärden. Two of the subbottom profiles indicate that the erosion is caused by SE to NW currents, likely related to short-term sea-level fluctuations caused by atmospheric air-pressure differences across the Baltic Sea. Many of the subbottom profiles from the area show signs of acoustic turbidity in the recent deposited sediments, indicating presence of shallow gas. The gas is assessed to be mainly of a biogenic origin but presence of reasonable amounts of gas with a thermogenic origin can at this stage not be ruled out.

Table of Contents

1 Introduction

This project is a marine high resolution seismo-acoustic study and a synthesis of sub-bottom profile and core-sample data gathered over four years (2008-2011) by students at Stockholm University. The author participated in the data collection in 2010. The acoustic sub-bottom profiling data are interpreted for the seismio-acoustic units and sediment cores are used for the geological interpretation. The project area (Figure 1) is located about 30 km south of Stockholm in the Trosa Archipelago, also referred to as the Södertörn region. The larger islands of Askö and Fifång define the southern and eastern borders of the project area while the lighthouse on Svarthäll and the islands Ljungholmen, Lustgården and Boknö-Oxnö defines the northern and western ends. In total this adds up to about 24 km^2 of which about 12 km^2 is covered in this project. The area is relatively exposed from the southeast where only small islands shelter Asköfjärden from the Baltic Sea. Other than this it is protected from the outer sea but exposed for winds from the larger fjards of the inner archipelago in the north. Askö with its surroundings consist of several natural preserves and together with the Askö Laboratory run by the Stockholm University Marine Research Centre, the region is a valuable resource for all areas in marine based research.

The surveys 2008-2011 were all carried out in a specific area in which permission to conduct marine geophysical mapping were granted by the Swedish military (Figure 1).

The aim of this work is to compile and interpret data collected from this area by Stockholm University. After an initial study of the data the three fields of focus were defined for the project; erosion-transport and deposition of sediments, sedimentological events tied to the last deglaciation and the accumulation and production of shallow gas in the area. The project aims were chosen to give a broad description of the seafloor properties near Askö laboratory, a region attracting attention from researchers and students from many disciplines. Parts of the study could be put into context together with other regions that during the last glaciation was affected in a similar way. An example of such an area is Ören located on the south-western parts of Torö about 5 km east of Askö, where a similar seismic study of the last glaciation and deglaciation was made by Jakobsson (1995). Furthermore the Geological Survey of Sweden (Sveriges Geologiska Undersökning, SGU) has made extensive seismic studies of the project area and its surroundings.

Since this paper has several different focus points that due to project extent limitations each may not get the attention they deserve, the main goal is to stimulate discussions on future studies of these focus points in the Askö region. The literature referred to have been selected in terms of relevance to each field of study but with certain reservations that some relevant publications may have been overlooked.

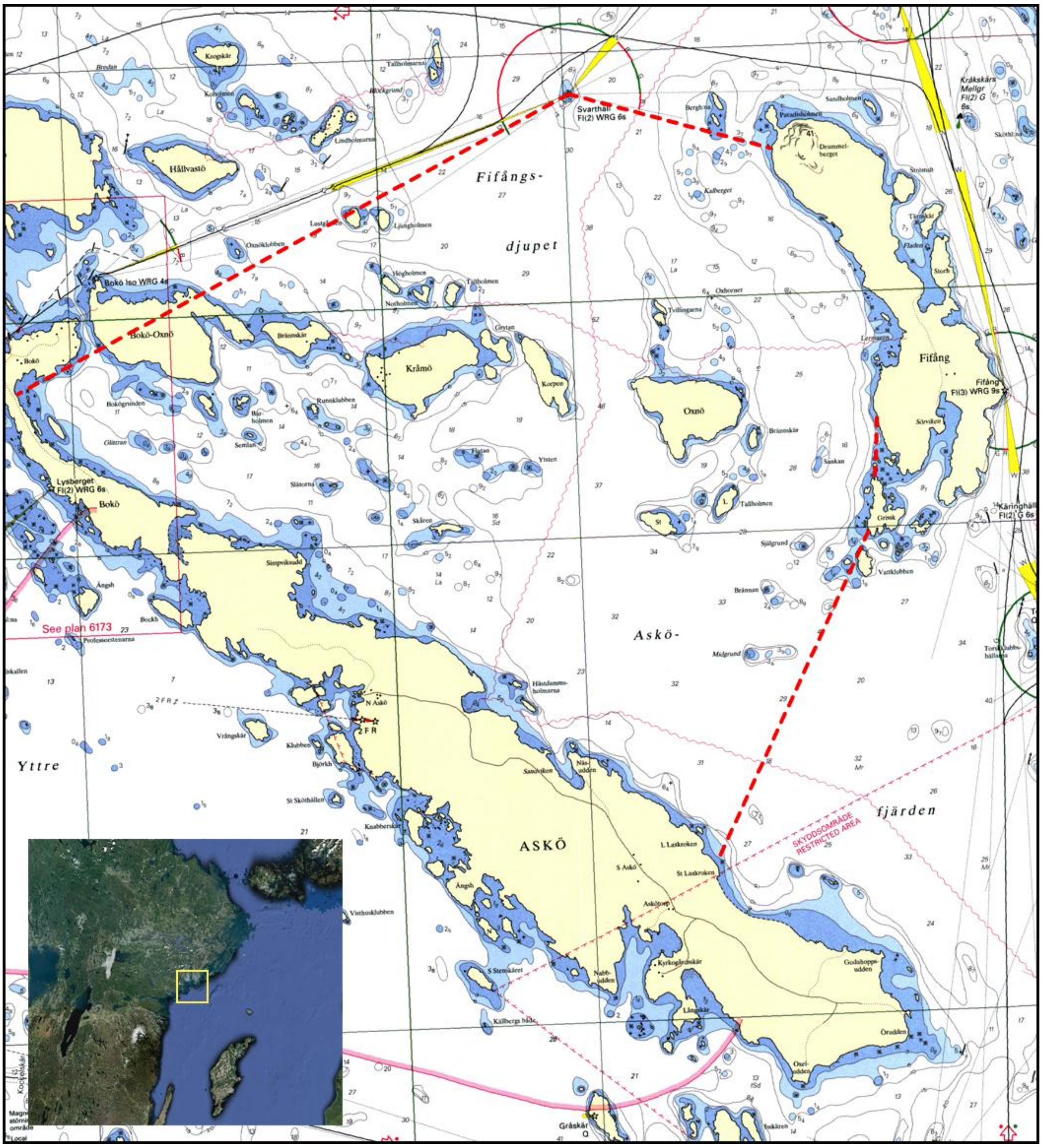

Figure 1: Map of project area. Red dashed lines marks the area within which seafloor mapping can be conducted and data may be openly handled and interpreted. From Sjöfartsverket sjökort LANDSORT 6172 and Google Earth.

2 Background

2.1 Geology

This brief description of the Geology in the area is mainly based on the scale 1:50 000 bedrock-, marine-, quaternary- geological and paleo-shoreline reconstruction maps from the Geological Survey of Sweden (SGU) available on the internet (http://maps2.sgu.se/kartgenerator/maporder_sv.html).

The quaternary geology map (In GSD-Terrängkartan. Lantmäteriet. MS2009/08799) reveals many traces of the last deglaciation on the islands within the project area. However, the area is dominated by crystalline bedrock. The sediments are generally restricted to streaks of local extensions. Comparisons with the topographic map (Lantmäteriet/Swedish Cadastral Service, Sweref – Terrängkartan, Nynäshamn, sheet 595) clearly show that the sediments are restricted to sheltered positions as valleys or crevasses. This would be expected since the area is relatively exposed. Glacial clay and wave washed sediments are the dominating components in the area and they are present on all islands except Oxnö where only wave washed sediments are present. A large deposit of wave washed sediments is present in the southern part of Askö. Somewhat further to the northwest on the island, postglacial sand deposits are present, which are almost unique for the region. These sediments were most likely deposited during the deglaciation of the southernmost Middle Swedish ice marginal zone in Younger Dryas, (Persson 1983; Brunnberg 1995). This is further described in section 2.2.1.

Based on the bedrock geological maps (In GSD-Terrängkartan. Lantmäteriet. MS2009/08799) the islands generally consist of svecofennian felsic intrusive rocks (Fredén 2009). On Askö there are also elements of partly migmatised rocks of volcanic and sedimentary origin (Fredén 2009). Furthermore, there are subsea streaks of ultramafic and intermediate intrusive bedrocks in Asköfjärden and at the western end of Fifångsdjupet. Some streaks cross the island Bokö-Oxnö. They all line up along the Southeast to northwest direction. On northern Bokö in the west there is also a short streak of carbonate rich sedimentary rock.

According to shoreline reconstructions from SGU (In GSD-Terrängkartan. Lantmäteriet. MS2009/08799) the northern parts of Fifång were the first to emerge from the water at 6000BP. Around 1000BP the entire area was more or less emerged.

2.2 Previous works

2.2.1 The last deglaciation

The Last Glacial Maximum (LGM) of the Weichselian glaciation occurred around 22 000 yearsBP. At this time the ice sheet reached as far southwards as to the northern parts of Germany and Poland thus entirely covering the Swedish mainland (Fredén 2009; Lokrantz & Sohlenius 2006). As the climate improved, the ice margins in northern Europe began to retreat. The deglaciation on the Swedish mainland started at around 16000 yearsBP when the ice margin reached the south-western coastal areas (Fredén 2009).

The present area is part of the Middle Swedish ice marginal zone and was most probably covered by ice during the climatic deterioration of the Younger Dryas stretching from around 12900 to 11700years BP (Rasmussen et al. 2006.). Brunnberg (1995) presents an ice margin reconstruction, based on his summary of the clay varve chronology in eastern Sweden. He demonstrates that the Södertörn area was covered by ice 11500 clay varve years BP. If adjusting the clay varve years by +760 according to the work of Andrén et al. (1999, 2002), this corresponds to 12260 cal. y BP, but is dated older in Fredén (2009) at 12600 cal. y BP. Fredén (2009) illustrates the area as ice free at 11500 cal. yBP.

The Younger Dryas cold climate gave rise to several stagnation zones (Persson 1983) that together make up the Middle Swedish ice marginal zone. Along the east coast, there are several features described by Persson (1983) where sorted material is overlain by several meters of till, which indicates a retreat followed by advance of the ice margin (Lundqvist 1995; Brunnberg 1995). A stable ice sheet, i.e. no annual net loss in mass, generally produces glaciofluvials and lodgement till near the ablation zone during the melting season. The glaciofluvials can consist of silts and sand and even coarser material transported through meltwater channels within the ice sheet, the lodgement till is compact material deposited underneath the ice during the melting season. Distinct signatures of a receding ice are terminal moraines, which are lodgement till overlain by ablation till, and large glaciofluvial deltas. The receding ice front deposits ablation till as it melts. As the ice front recedes further away, sorted materials transported by fluvial processes from the melting ice are deposited. Large glaciofluvial deposits overlain by terminal moraines are therefore a probable evidence of a second glaciation or re-advance of the ice sheet.

During the climatic improvement that followed Younger Dryas, the ice margin receded further north across the Swedish mainland at a steady pace. As the ice margin passed Mt. Billingen in Västergötland it triggered the final drainage of the Baltic ice lake, releasing around 7800 km^3 of freshwater into the ocean and lowering the sea level of the Baltic by 25 m (Jakobsson 2007). Andrén et al. (1999, 2002) date this event to around 11560cal. y BP. Most likely, the event had a notable impact on the sedimentation in the Baltic Sea.

The presence of glaciofluvial sediments overlain by till, together with exposed glaciofluvial deposits, are used by Persson (1983) to reconstruct the location of the southernmost part of the Middle Swedish ice marginal zone along the east coast. In the present area it extends from Hånömogen, past the south-eastern tip of Askö, up and including Ören and then continues in a north-easterly direction. This makes the Askö-Fifång area interesting, but also complicated to study as described by Brunnberg (1995).

2.2.2 Erosion and deposition in the Stockholm archipelago

Whether sediments are transported or deposited in a marine environment is mainly controlled by the grain size of sediments and the energy induced by external factors affecting the bed shear stress, i.e. the current velocity (Boggs 2006, pp. 27-29). The processes capable of seafloor erosion in this setting are limited to mass wasting events, wave action, or strong bottom currents. Mass wasting is not likely to have occurred in this area as there are no indicators such as slide scars or debris lobes. All signs of sea floor erosion occur in relatively flat areas. Wave erosion of the seafloor can only occur in shallow environments where the wave base reaches the seafloor, typically where the water depth equals half the wave length (Reading & Levell 1996).The typical wave length in an area is much depending on the fetch, i.e. the surface length of open waters which can be affected by wind (SMHI, Vindvågor 2009). Håkansson and Bryhn (2008) present a relationship between fetch lengths and water depths based on theoretical calculations. They estimate an average wave base of ~44 m and a maximum depth of erosion/transport of ~29 m in the Baltic Proper. As the Södertörn region is more sheltered compared to the open sea, and the fact that deposition occurs within the project area at depths <25 m in open locations and ~10 m in sheltered, the depths given by Håkansson and Bryhn must be considerably reduced for the present survey area.

Jonsson et al. (2003), in a report from Naturvårdsverket, explain in detail the mechanics and background of erosion, transport and deposition of sediments in the Stockholm archipelago. In this paper, the deposition and erosion/transport mechanism is presented in a similar manner as by Jonsson et al. (2003).

2.2.3 Gas accumulation in the Stockholm archipelago

The occurrence of gas in archipelagic environments, specifically in the Stockholm archipelago, has been a subject for research at Stockholm University for many years. This research is valuable for the discussion of ongoing processes in the project area. Gas charged marine sediments produce very prominent seismic features and are normally clearly visible in subbottom profiles. Mainly two different producers of gas are described in the various articles on the subject, biogenic and thermogenic. An isotopic relationship analysis of the ^{12}C and ^{13}C can be performed to determine whether the gas is of either kind (Söderberg & Flodén 1989; Laier et al. 1996). Biogenic gas production is estimated as being the most common source of methane in the shallow seas all over the world (Fleischer et al. 2001). This type of gas is produced by archaebacteria which under anaerobic conditions reduce specific substrates to produce methane as a by-product (Floodgate & Judd 1992). Parkes et al. (1990) show that these bacterial processes can occur, in some places, down to at least 80 m below the seafloor.

The term thermogenic gas is here used for the form of sediment migrating gas associated with tectonic lineaments. Thermogenic gas has previously been frequently observed in areas with underlying sedimentary bedrock (Hovland & Judd 1988). Investigations in the Stockholm archipelago show that thermogenic derived gas in the sediments is not exclusive for sedimentary bedrock areas (Söderberg & Flodén 1989). Thermogenic gas may also occur in areas of crystalline bedrock, as along the Swedish east coast. The gas is indicated to derive from deep within in the Earth's crust, escaping to the surface along major tectonic lineaments (Söderberg & Flodén 1989). Flodén and Söderberg (1994) present several types of migration models which explain how this gas seeps through the sediments under various circumstances.

Thermogenic gas seeps in the Stockholm archipelago are in many cases closely connected with circular depressions in the sediments called pockmarks. However, an enhanced production of biogenic gas normally occurs in areas of thermogenic gas seeps. Thus, the pockmarks are formed from the outflow of gas bubbles of a high biogenic origin. Accumulations in the sediment of pure biogenic gas are on the other hand not normally associated with pockmarks (Söderberg & Flodén 1992). There are also examples of areas where pockmarks with a thermogenic signature have been observed one year but a few years later in a following investigation of the area there were no longer indications of pockmark development (Söderberg 1993).

3 Methods

The high resolution seismo-acoustic recordings used for this project were shot in the period 2008 - 2011 from the Stockholm university research vessels Limanda and Aurelia as part of the course Marine Geoscientific Reasearch Methods. The course also included sediment corings and measurements of the water column temperature. Locations are given in Figure 2 and Figure 4.

The visual core descriptions, water column data, and information on methods referred to in this paper, are based on information given in the reports written by the students at the end of the courses. These reports are here referred to as the “Askö reports”. Even though the data and samples were obtained through the span of 4 years, the instruments and methods used were the same.

3.1 Data collection

3.1.1 Sampling

A standard Kullenberg sampler (piston corer) with a maximum sample depth of 3 m was used for the coring.
The cores were cut into 150 cm sections and marked with the year and consecutive numbers representing the coring site. The GPS position of each sampling location was noted.

The cores were visually described and their physical properties measured, using the multi sensor core logger (MSCL), at the Stockholm University. The metadata from the MCSL cannot be presented in this report since the data is either missing or not organized in a way where the individual cores can be matched to the results. Instead, the core descriptions presented here are based on the descriptions and interpretations from the Askö reports, which in its turn are based on the MCSL results. The original descriptions and MCSL results are available in the Askö reports (2008-2011).

3.1.2 Sound velocity

The sound velocity used for depth calculations in the subbottom profiles is 1469m/s. This is based on the average value of 11 harmonic mean calculations which in its turn is based on the water column temperature measurements (Figure 3) presented in the Askö reports (2008-2011). For each year 2-4 measurements were conducted at different sites using a temperature probe. Values were noted at every 5 meters through the water column starting 0.5 m below the surface.

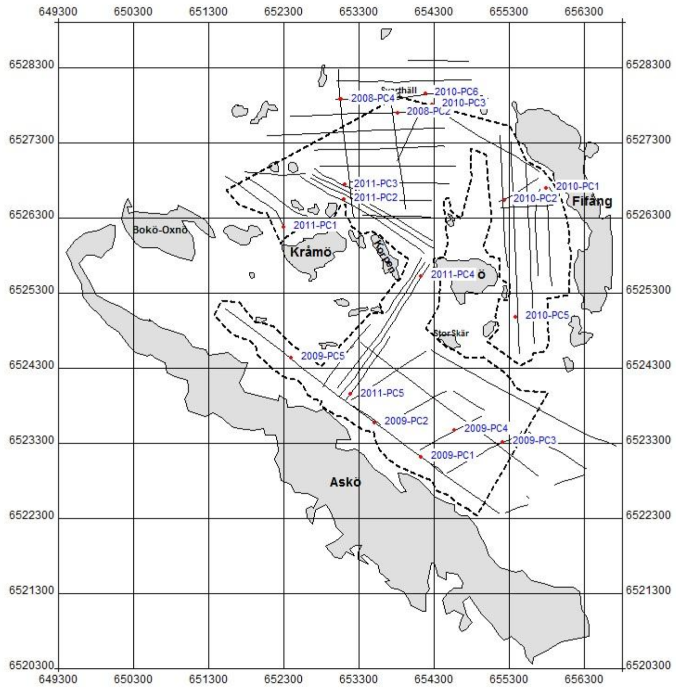

Figure 2: Samples taken 2008- 2011 marked with the annotations used in this project.

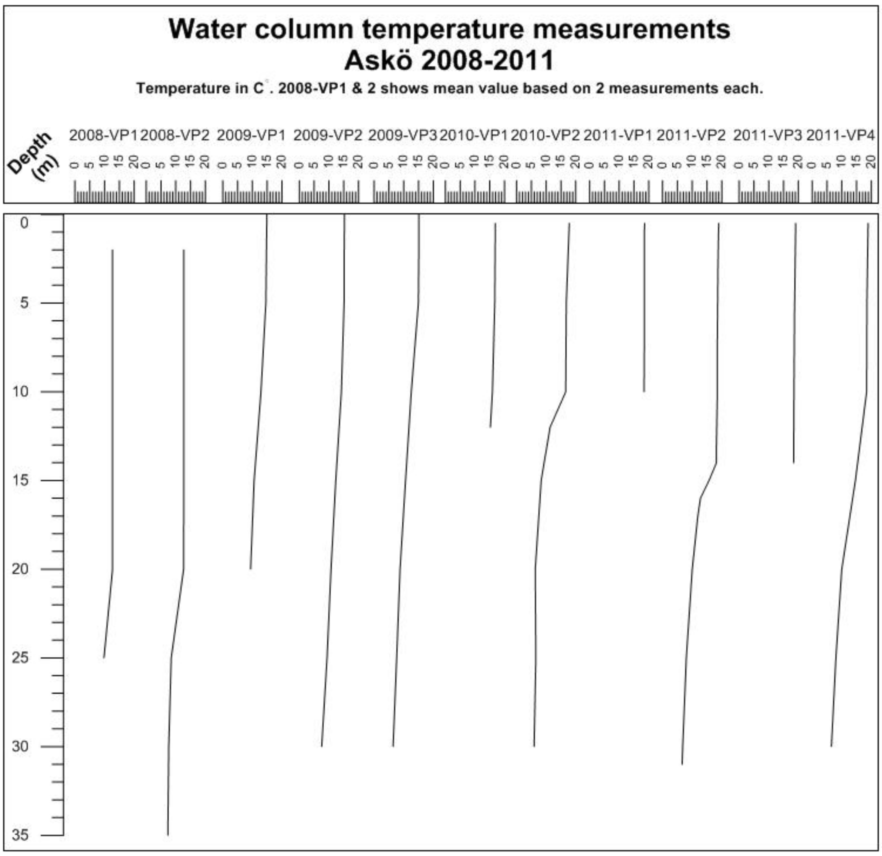

Figure 3: Graph over the water column temperature measurements on which the Sound velocity used in the project is based.

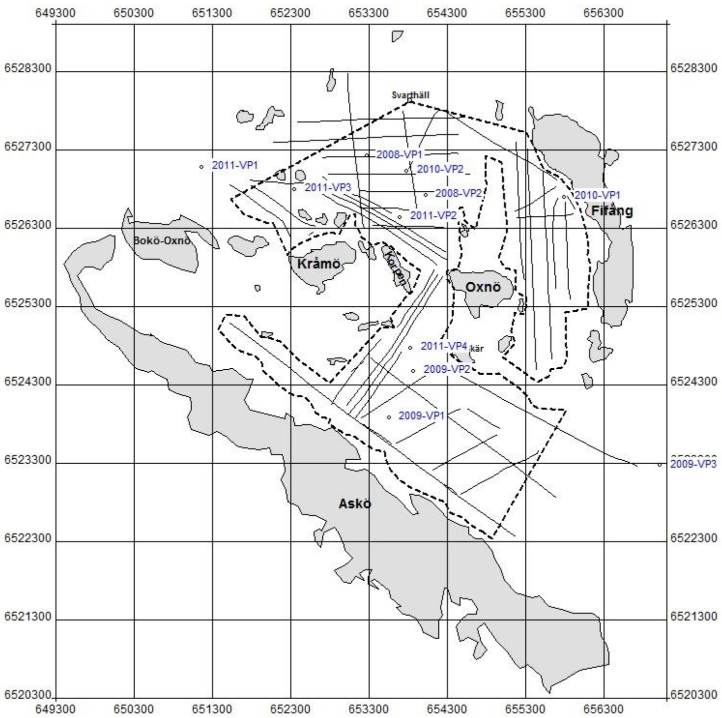

Figure 4: Water column temperature measurements conducted 2008- 2011 marked with the annotations used in this project.

3.1.3 Geophysical mapping

The seismic data interpreted here were collected with an Edge Tech Chirp Sonar SB-216S which is a towed, high resolution sub-bottom profiler capable to operate within a range of 2 – 16 kHz. Measurements using two echosounders operating at 24 and 28 kHz respectively, and one Sidescan sonar, EEG 260, were also recorded. The data collected with these units are not used in this report. In all subbottom profiling, there is a trade-off between resolution and penetration, as lower frequencies can penetrate deeper. The reason the chirp signal is preferred is that it, unlike the pingers, uses a pulse sweep across a frequency band and the received signal is decoded through matched correlation filtering (Schock et al. 1989). This yields a combination of good penetration and high resolution, and good signal-to noise ratio, which is of great advantage when surveying soft sediments. The range of frequency used for the Chirp Sonar was 3-9 kHz, i.e. a bandwidth of 6 kHz. The vertical resolution for a chirp signal equals PL x SS / 2. Where PL (pulse length) = 1 / bandwidth. This yields a vertical resolution of 12cm.

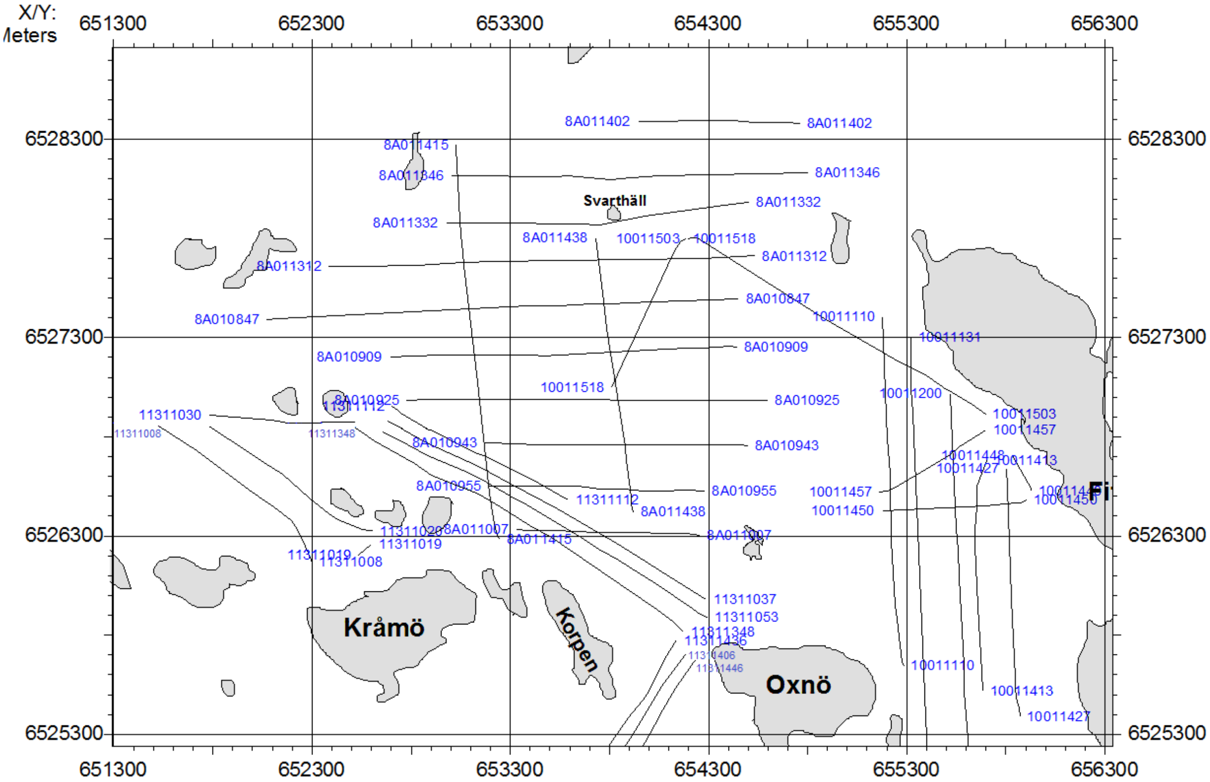

Figure 5: Overview of the northern project area and the track lines with their used annotations.

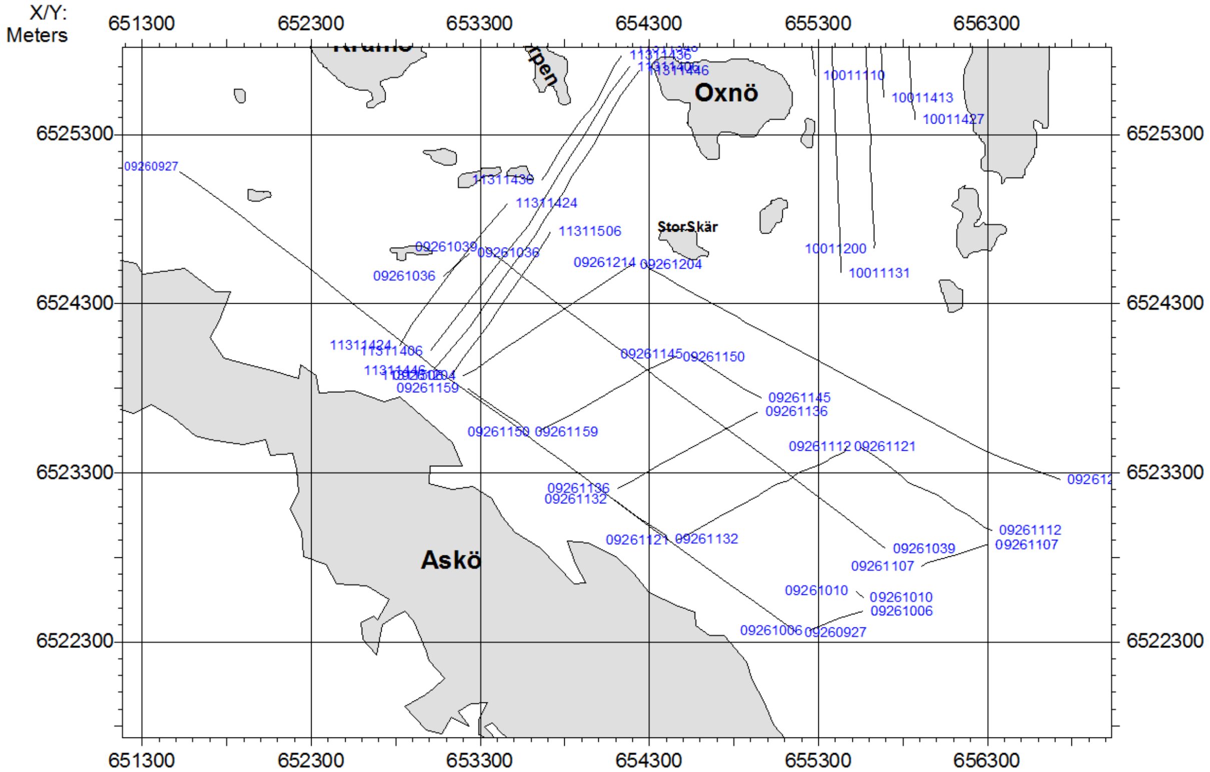

Figure 6: Overview of the southern project area and the track lines with their used annotations.

3.2 Data Processing

3.2.1 Import and processing of raw data

The interpretation software used was SMT Kingdom 8.7.1. The data were projected in Universal Transverse Mercator zone 33 and the coordinates were automatically read from the file-header of the SEG-Y file through bulk import of multiple files. SEG-Y files come in several different varieties and differ mainly in the architecture of the trace and file headers. Kingdom has some basic and optional criteria to be able to import a file containing seismic information.
The following criteria were met for importing files in this project:

- Survey name or line number
- Shotpoint information
- Coordinates
- Samples/trace relationship
- Sample interval

Since the seismic data was recorded in the custom Meridata .C08 format, some manual processing was needed to meet the criteria mentioned above. For further explanation on the import process, see appendix 1.

Data domains

Seismic data where imported with the time domain selected. The time domain was then converted to depth domain using SMT kingdoms *Trace calculations > Time<>depth conversion* tool. This allows a sound velocity to be specified and the seismic data to be viewed and interpreted with a vertical depth scale in meters rather than milliseconds.

3.2.2 Unit Interpretation

The acoustic stratigraphy was divided into seismic units separated by certain prominent reflectors. In SMT kingdom this is done by manual digitizing of prominent reflectors in the seismic view, referred to as horizons. In some areas the unit interpretations are more uncertain because of gas screening or other natural disturbances in the reflectors. Gas screening is quite common in the present area and is caused by the presence of methane gas in the sediments which disperses or absorbs the acoustic signal, causing acoustic turbidity (Hovland & Judd 1988; Judd & Hovland 1992). In gas screened areas the horizons were to some extent extrapolated, which is necessary in order to obtain a continuous unit interpretation later needed for the gridding process, see section 3.2.3.

Acoustic basement

The lowermost depth of acoustic penetration is in this work referred to as the “acoustic basement”. The high frequency sounder that was used for collecting the data is mainly used for penetrating softer sediments as mud and clay, so the impenetrable acoustic basement is normally made up of harder units such as glaciofluvial material, till, or even crystalline bedrock.

3.2.3 Gridding

Collection of seismo-acoustic data mainly yields distribution in two dimensions, X and Z or length, i.e. direction of travel, and depth. The density in Y, width, is determined by the distance between the seismic lines, which in practice will always be greater than the distance between each ping recorded in the travel direction. Since the data distribution is always denser in the X direction (direction of travel), a two dimensional plane will always have a dense variation (X) and scarce variation (Y) in the data distribution. Getting an overview over this kind of data in a plane perspective, such as shown in a map, is very difficult. Thus, a gridding process is used to connect data points in between the seismic lines and so binding them together allowing data interpolation to fill the areas which have no data by creating a grid.

Since the gridding process interpolates between the existing data points, the design of the gridding algorithm is crucial to the final outcome of the grid. The objective of the gridding process differs between projects and the methods of use are varying and dependent on the type and distribution of the

data. The main purpose of the grids in this project is to get a good overview of the data for interpretational and presentational purposes.
The gridding algorithm and its settings were mainly chosen with respect to the variations in spacing of the survey lines between different parts of the project area. Some areas have survey lines closer together while the southwestern parts in the area have a relative large distance between the survey lines.

For this project the grid algorithm “Flex gridding” in SMT kingdom was determined to best fit the criteria. Flex gridding allows the user to choose from, or combine, two different mathematical criteria, in SMT kingdom called Minimum Tension and Minimum Curvature. Additionally, levels of smoothness, ranging from minimum to heavy, is applied. Minimum Tension may be compared to a rubber sheet which is relaxed over the Z values of the grid nodes that contain data. It is based on the LaPlacian equation, a second-order partial differential equation. Minimum Curvature may be compared to a thin sheet of spring steel which is relaxed in a similar manner. It is based on the biharmonic equation, a fourth order partial differential equation (SMT Kingdom v.8.7.1 manual). The selected combination of equations is then applied to each grid node and the terms of the flexgrid algorithm affects 12 of its neighboring cells. In this manner all grid nodes are connected.
The grid algorithms and related equations are discussed by Hell and Jakobsson (2011). The uncertainties of grids are discussed by Smith (1993).

For this project the minimum curvature setting proved to be most applicable and was applied with the option for smoothness maximized. This option probably yields the most realistic interpolation in dense to scarce data sets as it weighs the depth of the neighboring data points higher, as opposed to the minimum tension algorithm which puts higher weights on the mean average of the entire data point set.

The smallest available grid cell size has been used to maximize the resolution for each grid. Since the final grids are only an assessment of the bathymetry there are uncertainties in the grid based interpretations. The grids were produced in the UTM zone 33 map projection, and used WGS 84 as both horizontal and vertical datum.

Grid constraints

As mentioned by Smith (1993), containments of grids help reduce the uncertainties of gridded data, and this is especially important for sparse datasets, which is the case in this project.
The grids are constrained by a polygon drawn to enclose the data sets, thus hindering gridding in areas far away from the survey lines where interpolations would be very uncertain. In total the polygon constrained area was 17.2 km^2, but the grids were cropped to 12 km^2, only showing the area approved for publication by the Swedish Armed Forces headquarters (Figure 1). To hinder the grids from interpolating through each other or on shallower depths than the seafloor, each grid was filtered with several grid calculation rules using the “extended math calculator” in SMT Kingdom, see Appendix 1.

The grids were also manually edited to remove smaller errors that the calculator constraint had missed. Some areas were also edited to give a more realistic appearance in terms of depth. To visually aid the manual editing, depth contours from a bathymetric map of the survey area were utilized (Flodén 2012). The bathymetric map is based on data from the same surveys as used in this report. The contours were created and manually edited using the software Surfer.

Gridding

A grid was created for each interpreted horizon and thus represents a defined seismo-acoustic unit. These grids were then constrained using the methods mentioned above. The final grids are used for interpretation of the sedimentation history and ongoing erosion of the project area. Isopach grids, which show sediment thickness, and depth grids, which show the depth below sea level of the seismo-acoustic unit, were created. The isopach grids are produced by comparing the vertical distance between two grids, the depth of the underlying grid is subtracted by the depth of the overlying grid. As an example, the total sediment thickness is the depth of the acoustic basement grid subtracted by the depth of the seafloor grid, yielding an isopach grid showing the sediment thickness in between. See Appendix 1.

The isopach grid over U1, see section 5.1.1, was used to create an overview map of the erosional/depositional areas in the software Global Mapper (see section 5.2). The depositional areas have been plotted in areas where U1 is thicker than 2 m. The erosional/transport areas have been plotted where the seafloor is made up of glacial mud or till/bedrock. Areas where the thickness of U1 is < 2 m have not been included with the depositional areas, this is because of the low sedimentation rate which could indicate that material is deposited annually when transport activity is low, and then swept away later in the season as the area shifts to a higher energy environment.

4 Results

4.1 Seismics

In general the chirp profiles are of good quality and acoustic units could be clearly distinguished, except for where gas screening occurs. In total 3 units with corresponding subunits where distinguished (Figure 7; Table 1), U3 with 2 sub units, U3a and U3b, U2 without subunits, and U1 with 3 subunits, U1a, U1b and U1c.

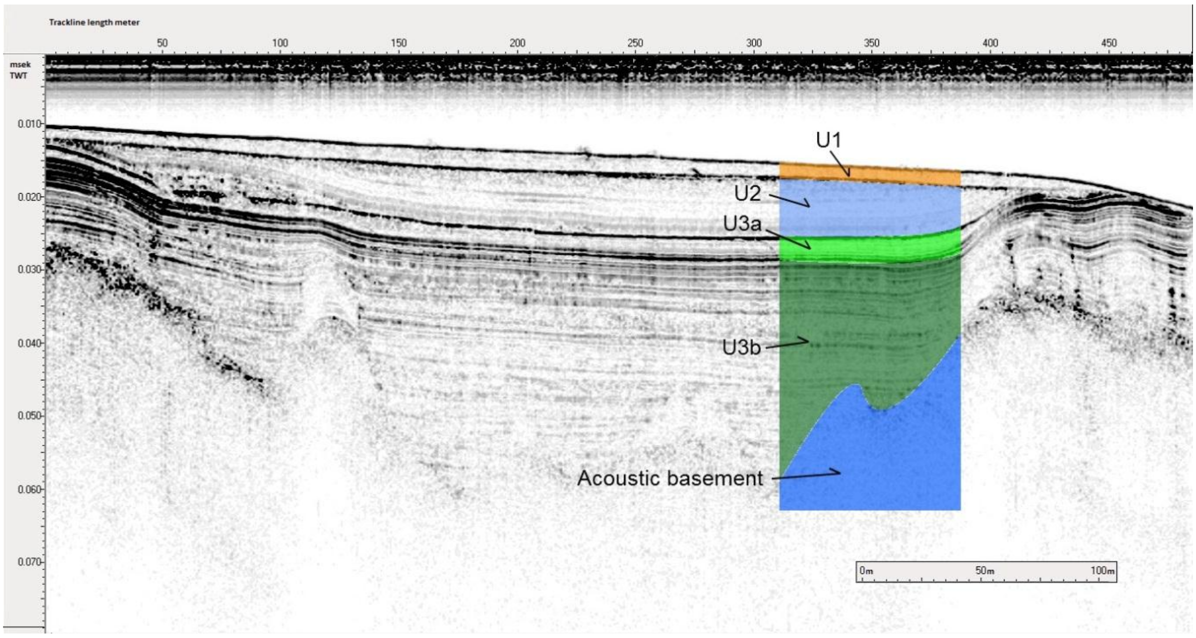

Figure 7: Chirp sonar profile 8A010847 with unit interpretations marked in color.

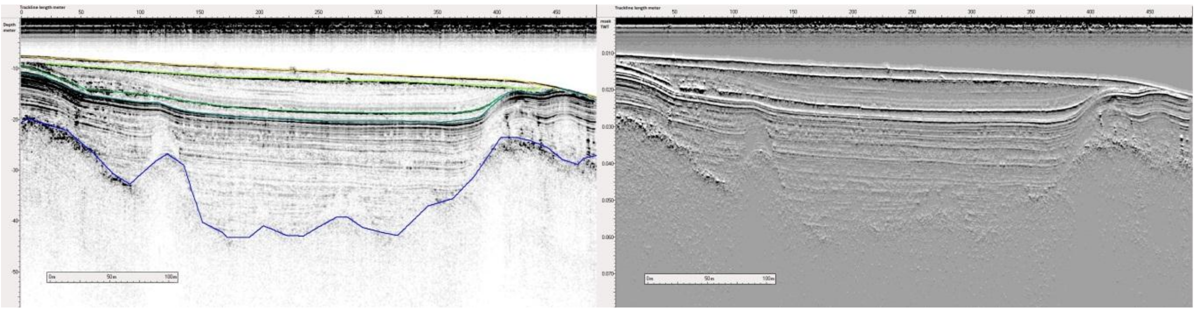

Figure 8: Chirp sonar profile 8A010847. Left image shows section with the interpreted horizons. Right image shows same profile in Hilbert filtering.

U3b is observed all through the area and is only absent where crystalline bedrock outcrops at the seafloor. This is also the thickest of all units both in average and maximum. The unit's lower boundary is always in direct contact with the acoustic basement and is characterized by alternating strong and weak reflectors defining layers of varying thickness up to several 10s of centimeters.

U3a is always overlying U3b and is present, with few exceptions, all through the area. The unit is rarely found in direct contact with the seafloor and is in some areas occasionally hard to identify. It is recognized as a relatively thin unit, 1-2 m, defined by strong reflectors at the top and bottom with several, relatively thin, weak reflectors in between.

U2 is in average the second thickest unit in the area and is characterized as a relatively uniform layer up to 10 m in thickness, sometimes with weak internal reflectors. It is generally overlying U3a but at some locations this layer appears to rest directly upon U3b. In most cases the latter is observed where the acoustic signal is weak or showing signs of dispersal but occasionally also in locations that show good seismic penetration.

U1b is a relatively uniform unit generally without any internal reflectors. It is of varying thickness and always observed overlying U2 and U3. The U1a unit denotes locations where there are signs of gas or adjacent to areas with signs of gas. The subunits U1a and U1b have a very similar signature in locations where U1b is not affected by acoustic disturbances. They do not drape the underlying units in contrast to U2 and U3 and are always the topmost units. They appear in the areas shown in Figure 13.

Subunit U1c is observed in only a few locations and is similar in its acoustic signature to U1a and U1b but appears in small banks and seems more resilient to erosion.

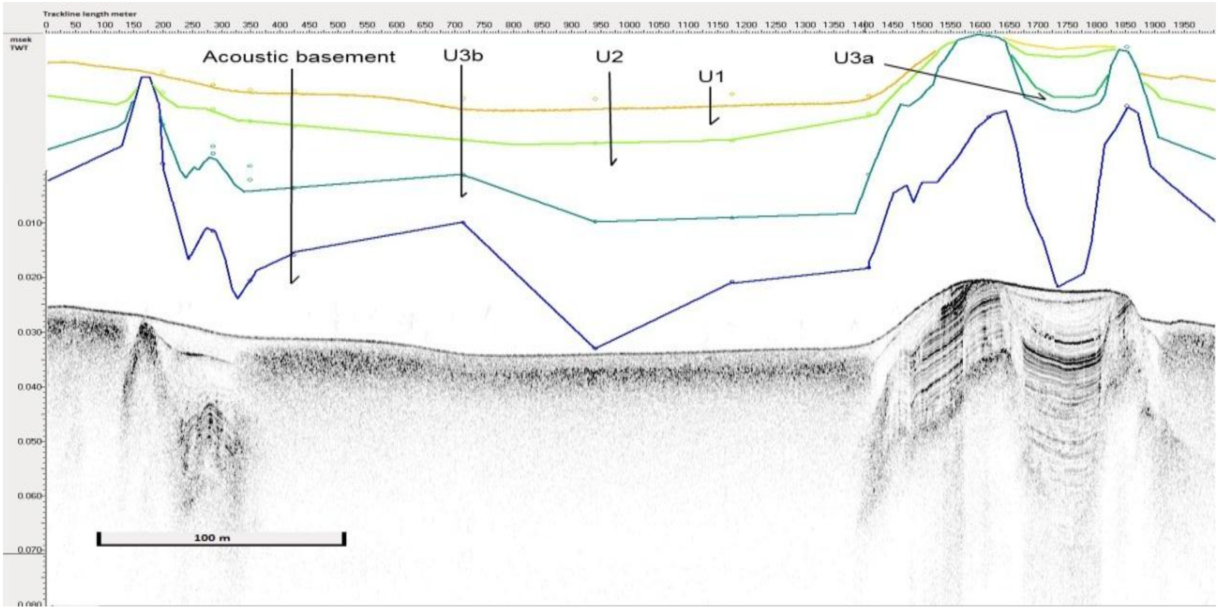

Figure 9: Chirp sonar profile 8A011415 in full length. Interpreted horizon with vertical offset.

Seismo acoustic Unit	Description Acoustic signature	Example
U1a	Top boundary is recognized by a distinct strong reflector. Internally most often diffuse without any underlying reflectors showing. In some places, often at each end of the unit, homogenous but occasionally with weak internal reflectors.	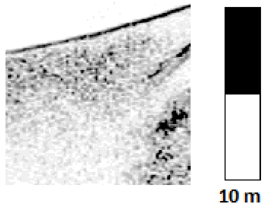
U1b	Relatively homogenous but occasionally with weak internal reflectors. Top and bottom boundary is recognized by relative thick strong reflectors. Does not drape the underlying units in contrast to U2 and U3. Always the topmost unit.	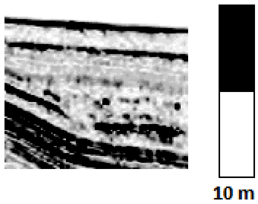
U1c	Weak or no internal reflectors. Where observed, always the topmost unit. Appears as small banks.	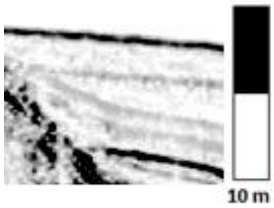
U2	In average the second thickest unit in the area, up to 10 m. Relatively uniform, sometimes with weak internal reflectors. Generally rests upon U3a but in some places it appears to rest directly upon U3b.	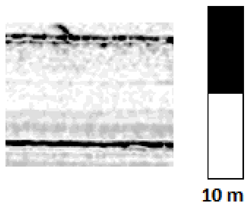
U3a	A relatively thin unit, 1-2m, defined by strong reflectors at the top and bottom with several, relatively thin, weak reflectors in between	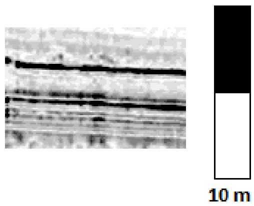
U3b	Bottom boundary is always in direct contact with acoustic basement. It is characterized by alternating strong and weak internal reflectors of varying thickness up to several 10s of centimeters.	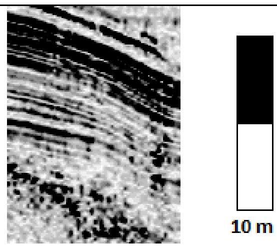
Acoustic basement	No internal reflectors and no bottom boundary. The top boundary is distinguished as a diffuse reflector varying from strong to weak in different locations.	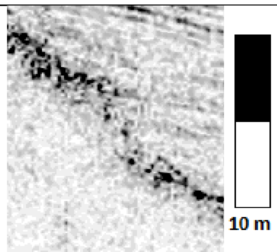

Table 1: Descriptions of the acoustic signatures of the units.

4.2Grids

To illustrate the area with aim at the project objectives three isopach grids and three depth grids are used. The isopach grids show the sediment thickness of U1 (Figure 10 left), U3 (Figure 10 right) and the sediment thickness from the acoustic basement to the seafloor (Figure 11), also referred to as the total sediment thickness. The isopach maps (Figure 10 and Figure 11) can be used to locate areas with tendencies for sediment deposition and erosion. The depth grids show the depth of the seafloor (Figure 12), U1 (Figure 13 left) and U3 (Figure 13 right). The sea chart with depth curves (Figure 12) can be used as a comparison against the seafloor depth grid. In addition, a 3D image of the sediment thickness (Figure 14) is presented in this section and a gridded marine geology map, showing the units propagation on the seafloor, is presented in section 5.1.

The distribution of available information varies over the project area. The track lines in the southernmost parts is relatively wide apart and relative large areas in some locations lacks information on underlying reflectors due to gas screening. These areas with sparse access to seismic information have a low precision in the interpretation while areas with good access, invariably along some tracklines, yield a high interpretational precision.

Because of the unequal access to information, the gridded surface is smoother in areas with less information and show spikes in areas with more information. This is particularly evident in Figure 14 where spikes similar to pinches in clay appear along some tracklines.

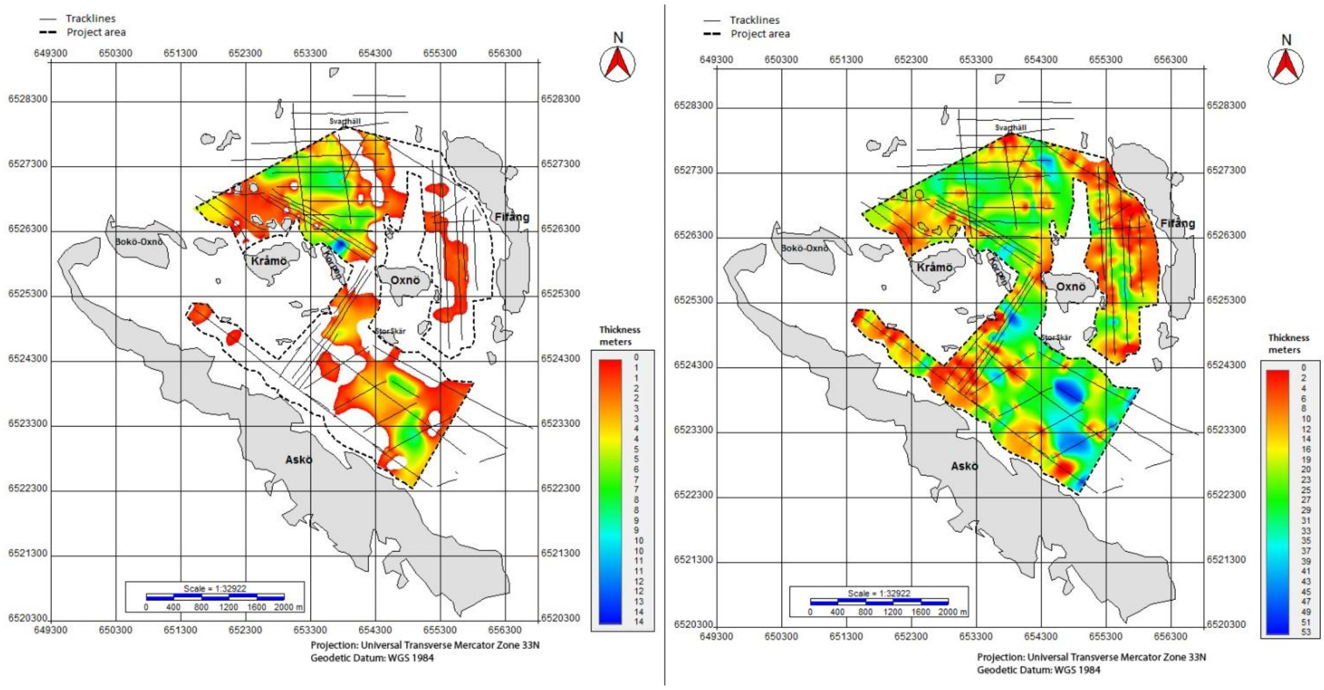

Figure 10: Left: Isopach of U1. Right: Isopach of U3.

Results from calculations of the gridded seafloor (Figure 12) shows that the area has a mean depth of 22.8 m and the total sediment thickness grid shows a mean total sediment thickness value of 18.9 m. From the seafloor grid in Figure 12, assumptions of the bathymetry of the area and its variations in depth can be made. Based on this, the deeper parts of the area are generally proximate to Asköfjärden and Fifångsdjupet, grounding in the cay and islet areas between Kråmö and Askö, west of Fifång and around the smaller islands in the western parts of Fifångsdjupet.

The narrow passage between Korpen and Oxnö makes the most prominent feature in the bathymetry of the area. With a maximum depth of 53 m it stands out from the surroundings but despite the great depth this location is not prominent on the isopach map over the total sediment thickness (Figure 11), measuring between 18 m and 25 m, almost equal to the mean depth of the area, 19 m. A shallower streak can be distinguished in the seafloor grid between Tvillingarna and Svarthäll in the northern half of the area. The total sediment thickness here is also relative thin.

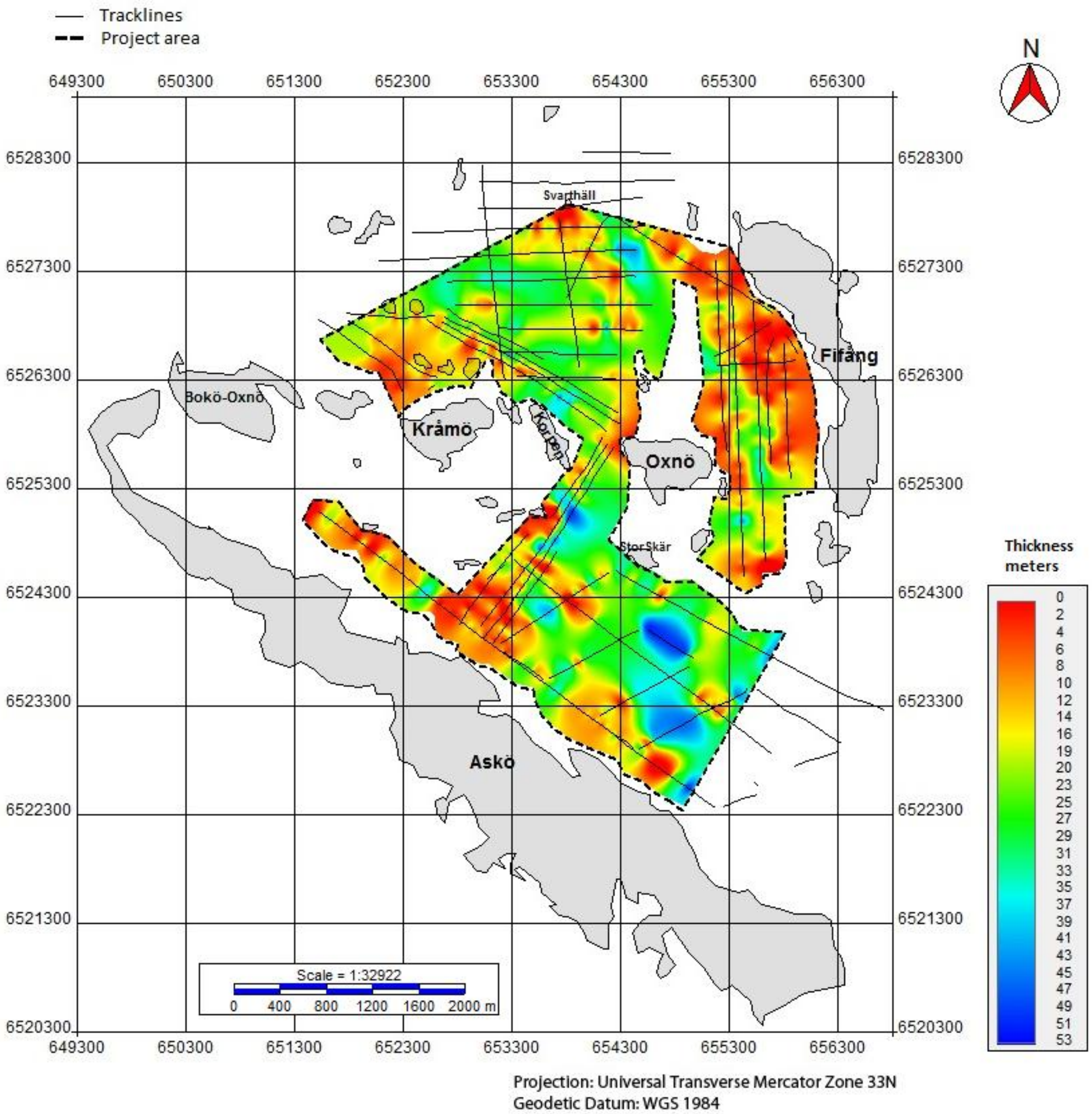

Figure 11: Isopach map illustrates the total sediment thickness of the area, measured from seafloor down to acoustic basement which generally consists of till or crystalline bedrock.

The U1 isopach map (Figure 10) over the presumably more recent deposits, indicates where sediments are presently being deposited and where they are not. Because of the relatively small extent of the survey area it is reasonable to assume a uniform sediment availability. The variations of thickness in U1 should consequently reflect variations in the depositional pattern. Areas with large amounts of deposited material thus indicate a low energy environment while white areas, which show complete absence of U1, indicate a higher energy environment. There is however a distinct possibility for miscalculation of the sediment thickness in the areas of high recent deposition since the profiles from these areas often are obscured by gas screening (See section 3.2.2). The U3 deposits, as seen in Figure 13, are present all through the area with only a few exceptions where the acoustic basement is exposed at seafloor.

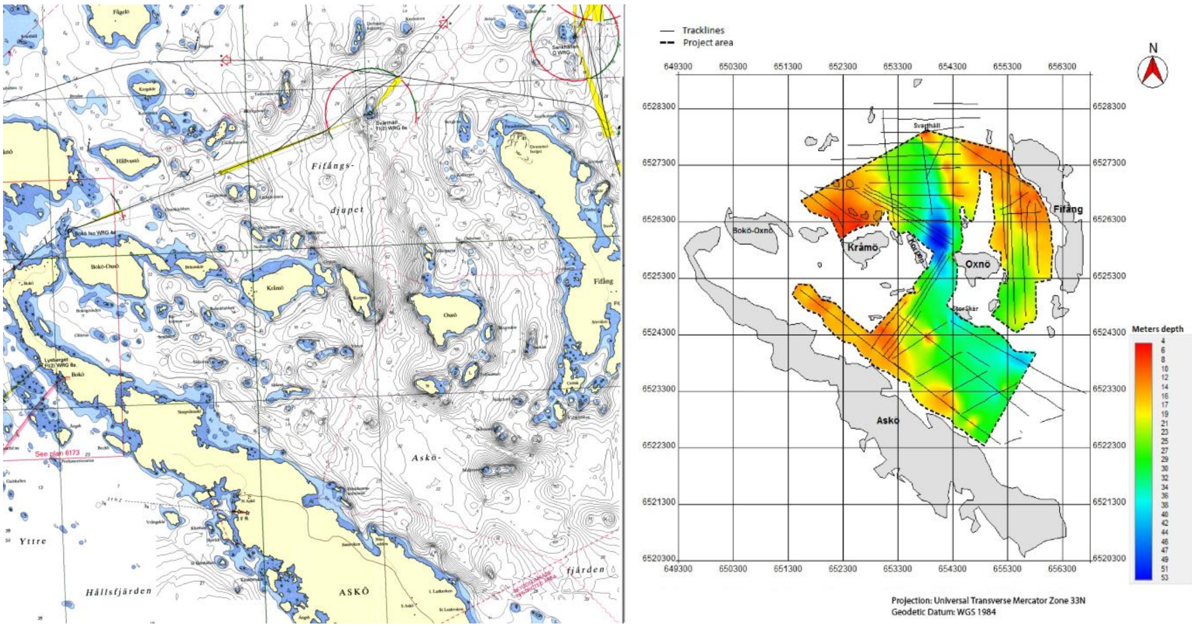

Figure 12: Left: Sea chart with depth curves provided (Flodén 2012). Right: Seafloor grid, depth in meters.

By comparing the isopach grids to the bathymetry of the area (Figure 12) differences in deposition in relation to depth can be pointed out. The total sediment Isopach grid in Figure 11 shows a reasonable relation between shallow areas and low sediment thickness, i.e. west of Fifång and along the Askö coast. The deeper areas, however, have a less obvious relation to high sediment thicknesses. Comparing the bathymetry (Figure 10) to the U3 isopach (Figure 10), the large depth to sedimentation thickness relation is even weaker. The U1 isopach shows a certain relation between low to no sedimentation thickness in shallow areas but there are also deep areas that have little or no thickness.

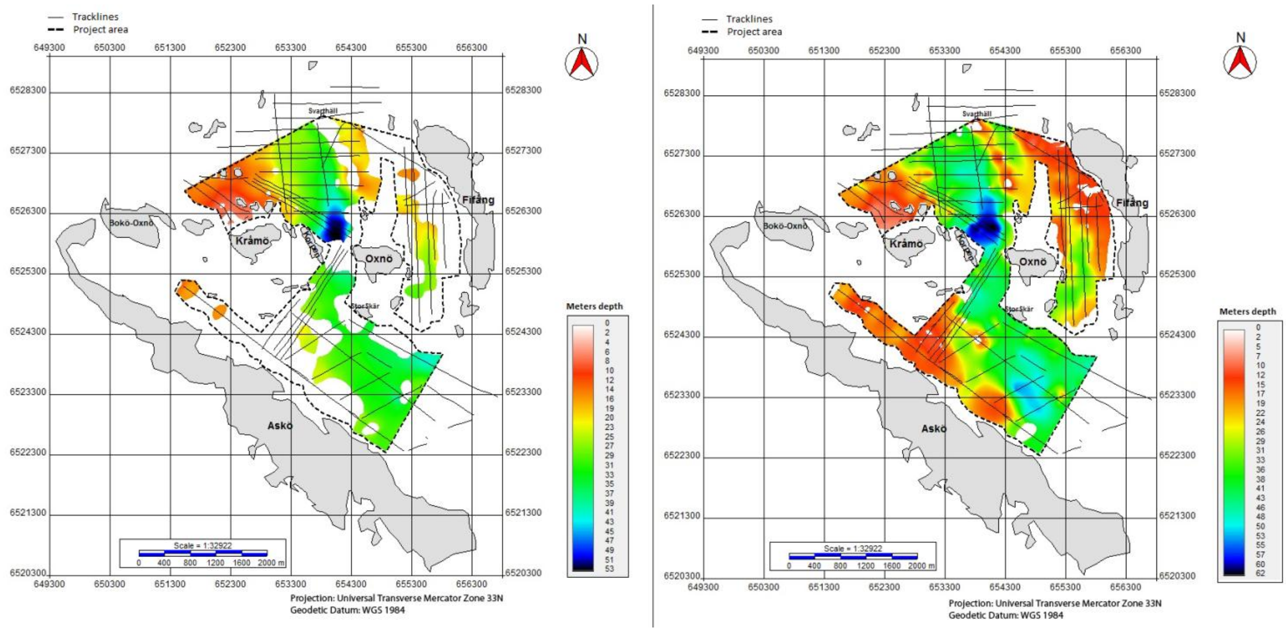

Figure 13: Left: Depth of U1. Right: Depth of U3

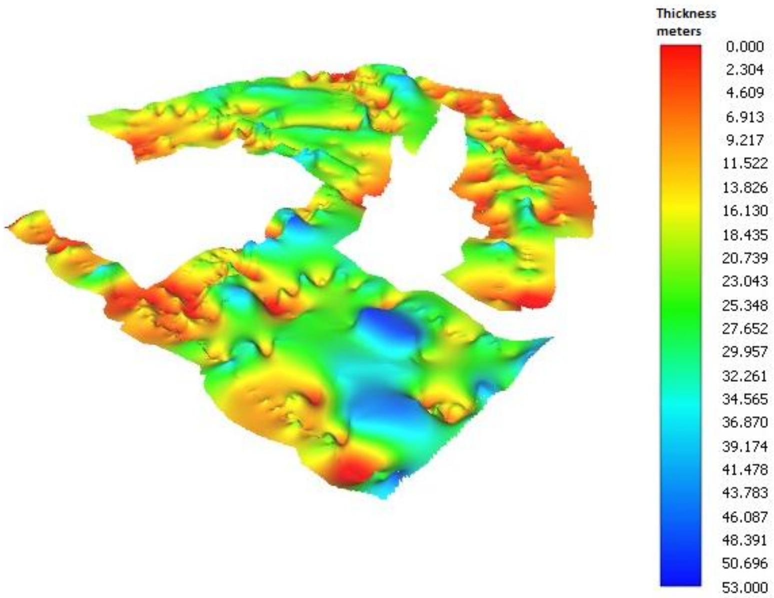

Figure 14: 3D image created with the kingdom software package Vupack showing the sediment thickness of the project area.

4.3 Sampling

In total 18 core samples were retrieved from the area. Four of these were selected from the Askö reports, 2010-PC2, 2010-PC3, 2008-PC4 and 2009-PC3. Their locations are marked in Figure 2 in plane and Figure 17-20 in profile. The cores in the profiles are marked with its actual starting depth and length. In some profiles they therefore appear to start some distance above or below the seafloor. This is because the sampling may not have been performed exactly on the trackline. The descriptions from the remaining cores have been analyzed but the results are only briefly discussed here, for more details about these samples the reader is referred to the Askö reports. The core descriptions here are a result from analysis of the interpreted lithology and descriptions in the Askö reports. The cores were selected from the subbottom profiles to be representative of the seismic units, U1a, U1b, U2, and U3b. Subunit U1c is not represented since it has no corresponding sample.

Short description (All levels are mentioned from the top of the cores):

2010-PC2
Homogenous grey to greenish grey clay overlaid by muddy clay and mud/ooze. Alternating darker grey layers and lighter grey/greenish layers downwards from 144 cm.

2010-PC3
Muddy clay with a black to grey color that shifts to brown to grey muddy clay at 29 cm. Smell of sulphur. Occasional organic material.

2008-PC4
Muddy first 10 cm with a sharp contact to bluish grey laminated clay graduating to brownish grey laminations downwards from 47 cm. Brown-grey laminated clay follows down to 186 cm where it shifts to around 15 cm thick beige layers which separates from each other by a sharp dark contact and the gradually becoming lighter.

2009-PC3
Grey laminated clay overlain by 10 cm mud. The laminations vary in thickness from 1 – 6 cm with dark grey color that gradually shifts towards light grey.

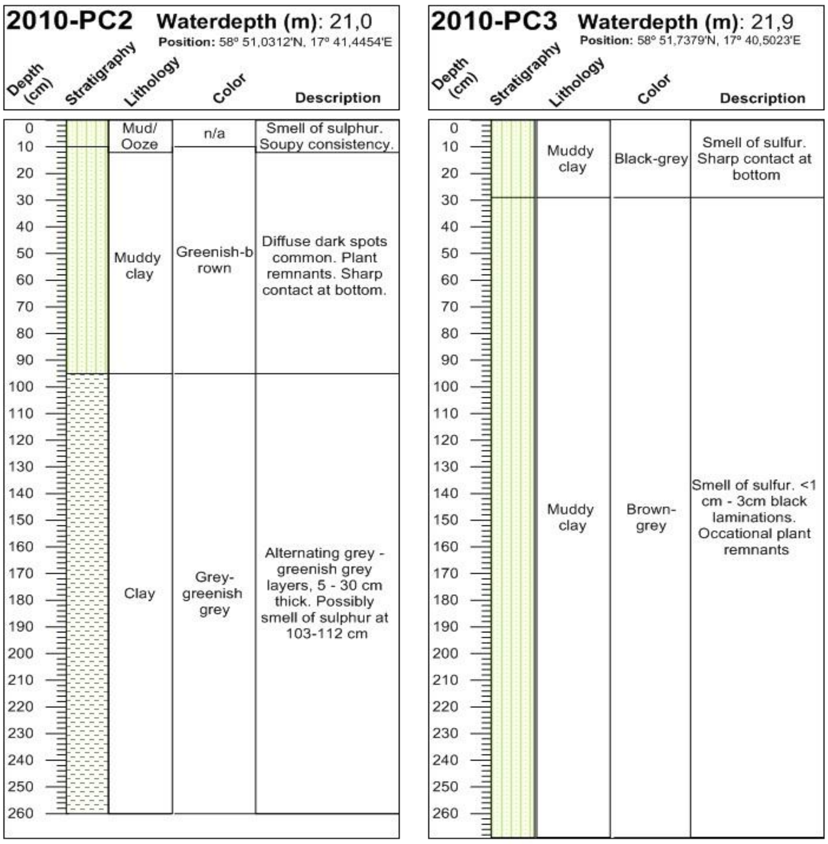

Figure 15: Lithology of core 2010-PC2 (left), and core 2010-PC3 (right)

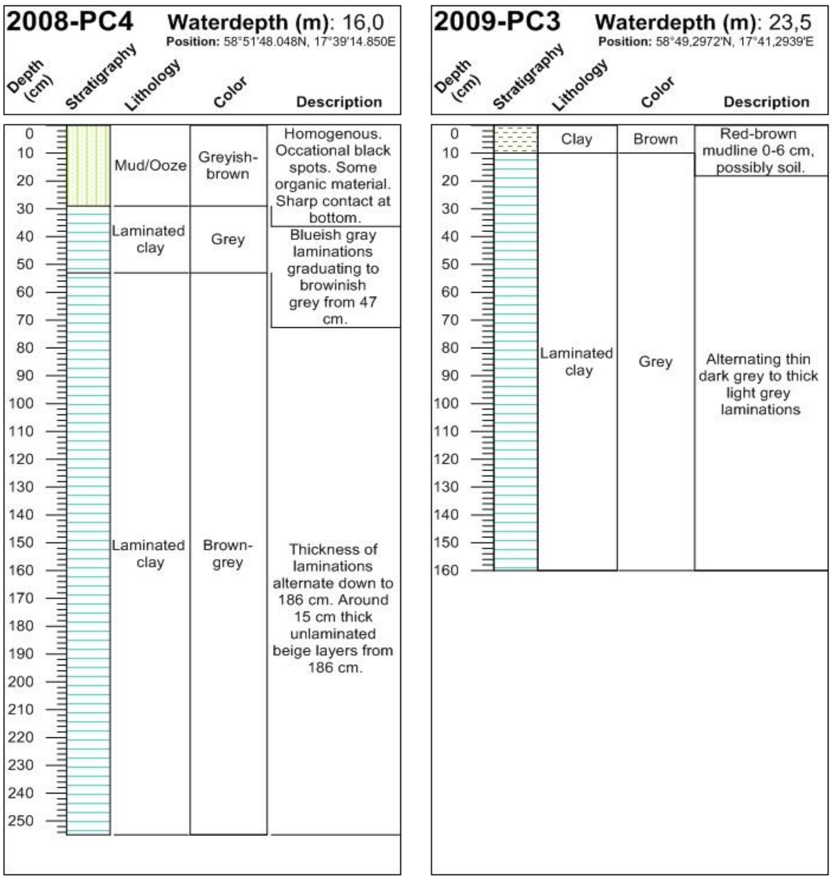

Figure 16: Lithology of core 2008-PC4 (left), and core 2009-PC3 (right)

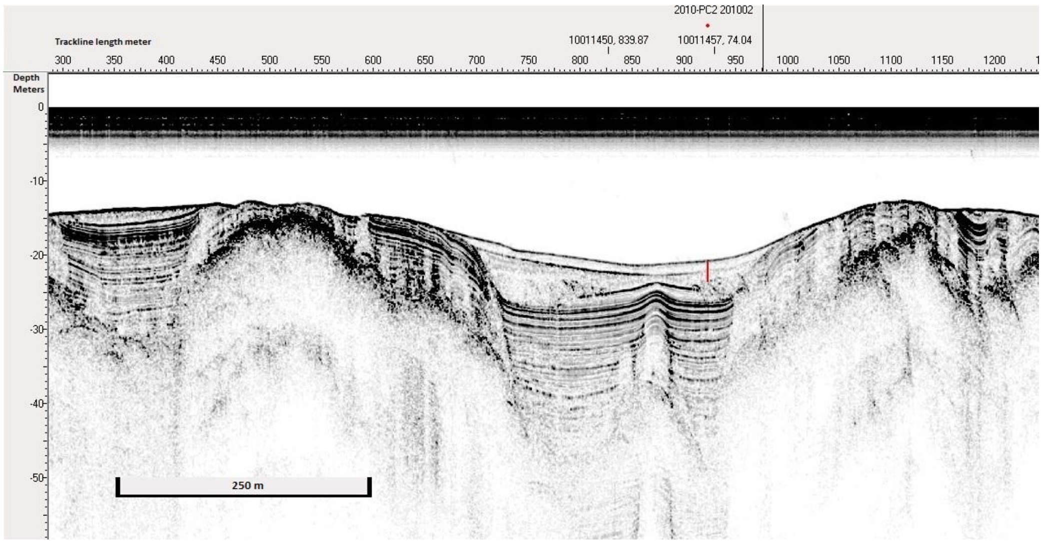

Figure 17: Subbottom profile showing location for 2010-PC2 marked in red.

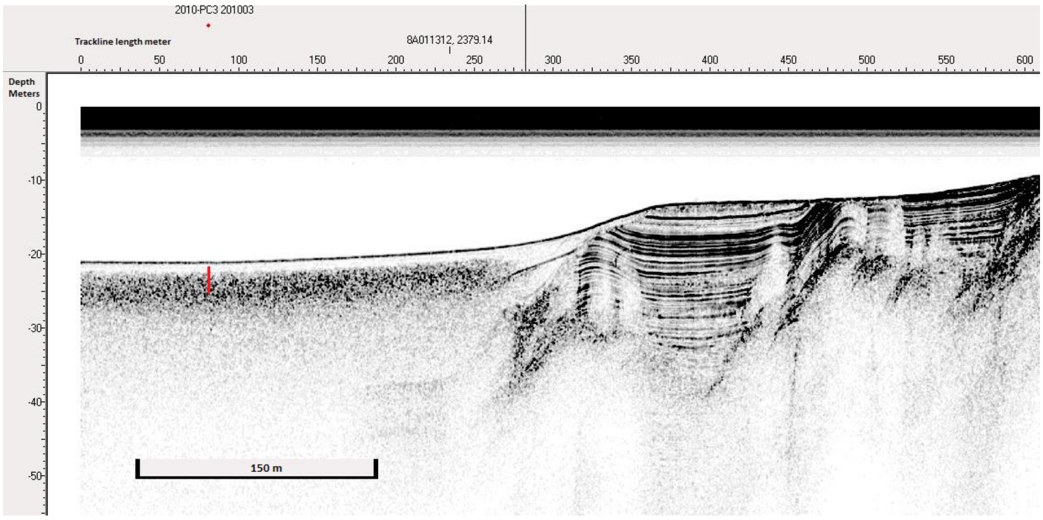

Figure 18: Subbottom profile showing location for 2010-PC3 marked in red.

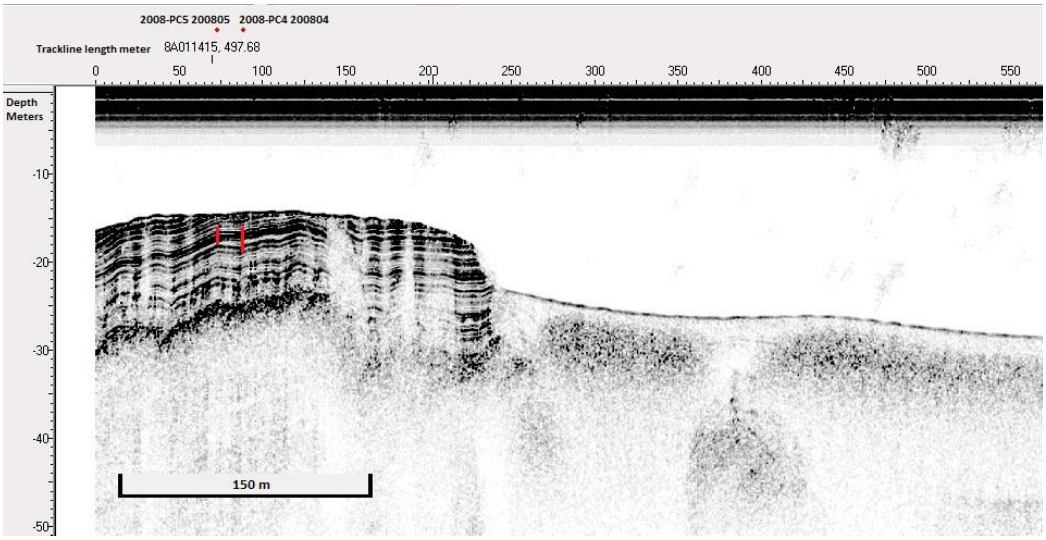

Figure 19: Subbottom profile showing location for 2008-PC4 and 2008-PC5 marked in red.

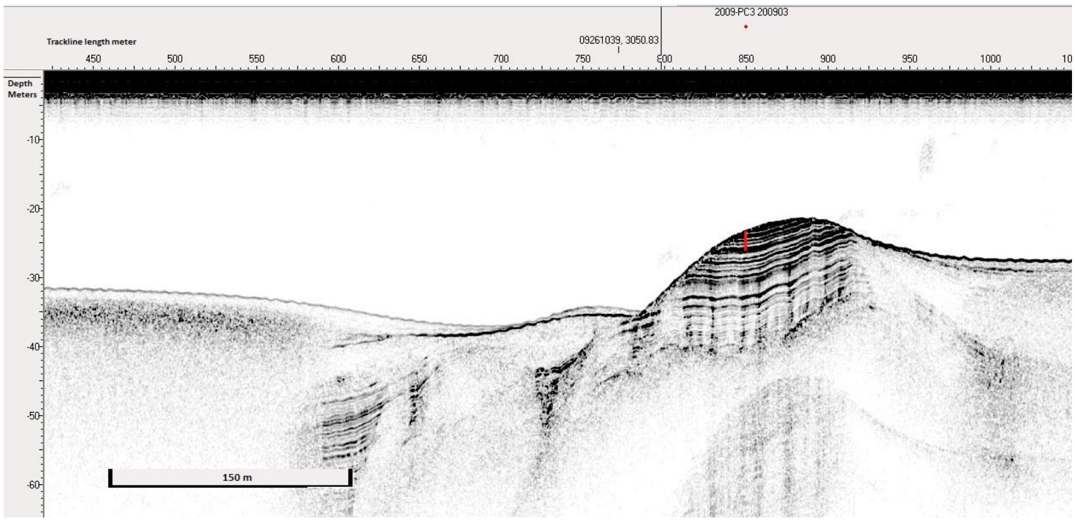

Figure 20: Subbottom profile showing location for 2009-PC3 marked in red.

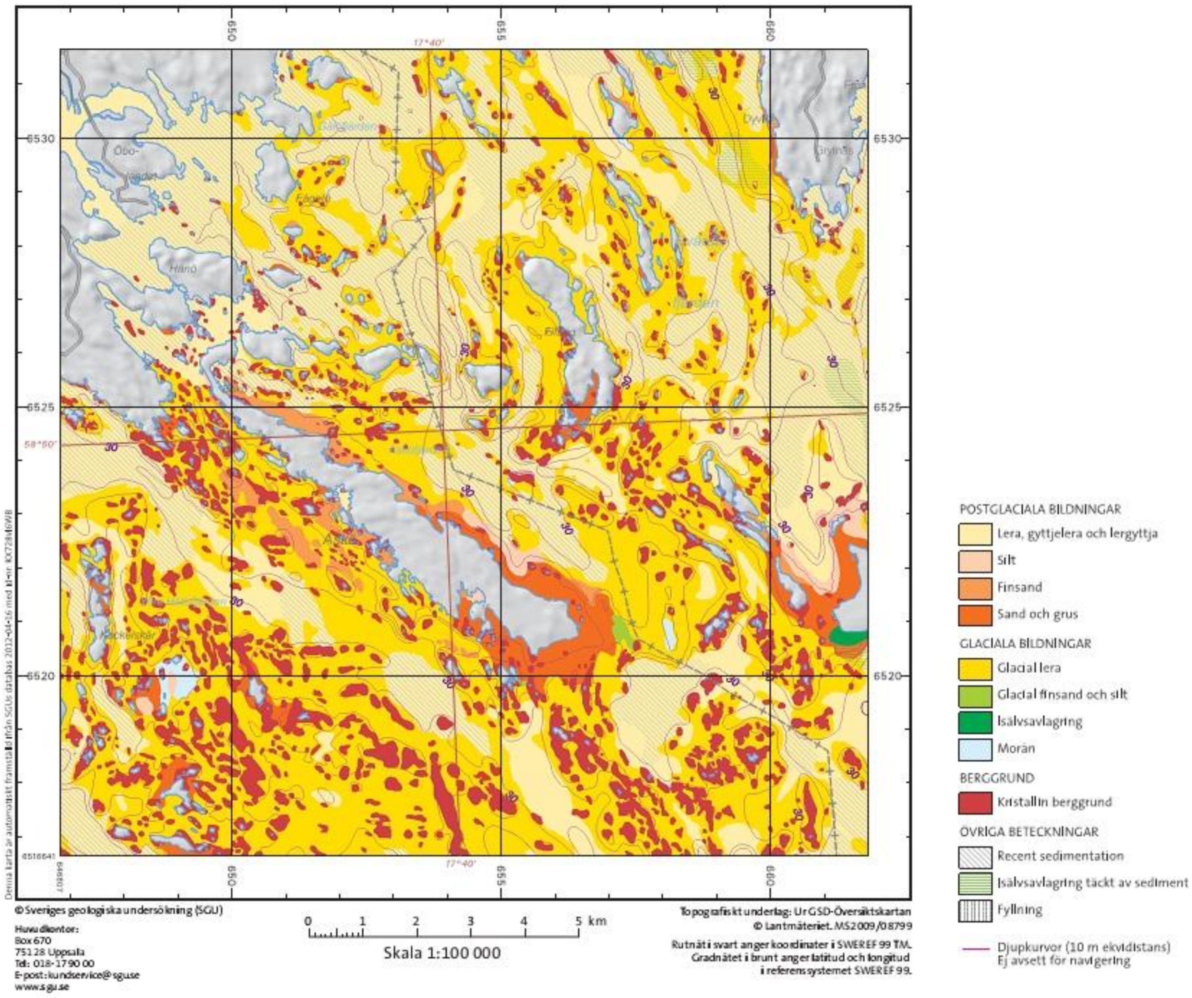

Figure 21: Marine geology map of the exposed seafloor sediments (In GSD-Översiktskartan. Lantmäteriet. MS2009/08799). The map is mainly based on hydroacoustic measurements.

5 Discussion

5.1 The sediment units

When correlating the subbottom profiles with the lithology of the cores (Table 2), three different events are distinguished. Each can be tied to one of the main seismo-acoustic units. Thus, U3 is interpreted as glacial clay, distally deposited from a receding ice, and U3a can possibly be distinguished from U3b in the lithology, see section 5.1.1 below. Due to the lack of laminations and low organic content, U2 is likely to have been deposited in an environment of large outflow of water and sediments. Conditions like these are characteristic for the time after the drainage of the Baltic Ice Lake (Björck, 2008), therefore U2 consists most likely of postglacial clay. U1, consisting mostly of mud, is part of the ongoing deposition in the area and referred to as a recent deposition. The subunits U1a and U1b cannot be distinguished in the samples, merely in the profiles. Their differences therefore seem to be tied to their acoustic signature which, in turn, may depend on variations in gas concentration. When comparing the depositional areas of U1c with the marine geology map (Figure 21), U1c probably consist of recent deposits of sand and gravel. Based on the remnant glacial deposits on the surrounding islands, mainly Askö, an assessment of the sediments below the acoustic basement can be made. The quaternary geology map from SGU (In GSD-Terrängkartan. Lantmäteriet. MS2009/08799) show wave washed sediments such as gravel and sandy till. Most likely these components form the acoustic basement, underlying the softer sediments in the area.

The grid map in Figure 22 illustrates the areas where the successive units are exposed at the seafloor and may be compared to the SGU marine geology map (Figure 21). However, the SGU map is mainly based on interpretations from Side scan sonar, which provides an acoustic image of the seafloor. Side scan data can yield better information about the seafloor sediments that have a characteristic surface, such as sand or gravel. It is however more limited when it comes to distinguish sediment types that are best characterized by their internal reflectors, such as un-laminated, postglacial clay. U1 is the dominating unit in both figures and is presented as a postglacial deposit consisting of clay, gyttja clay and clayey gyttja which concurs with U1 being a recent deposit. U2 on the other hand is not represented on the SGU map, but seems to correlate well with areas marked as glacial clay. The most notable difference is the passage between Korpen and Oxnö where the subbottom profiles shows exposed postglacial and glacial clay whereas the same area on the SGU map is marked as being recently deposited.

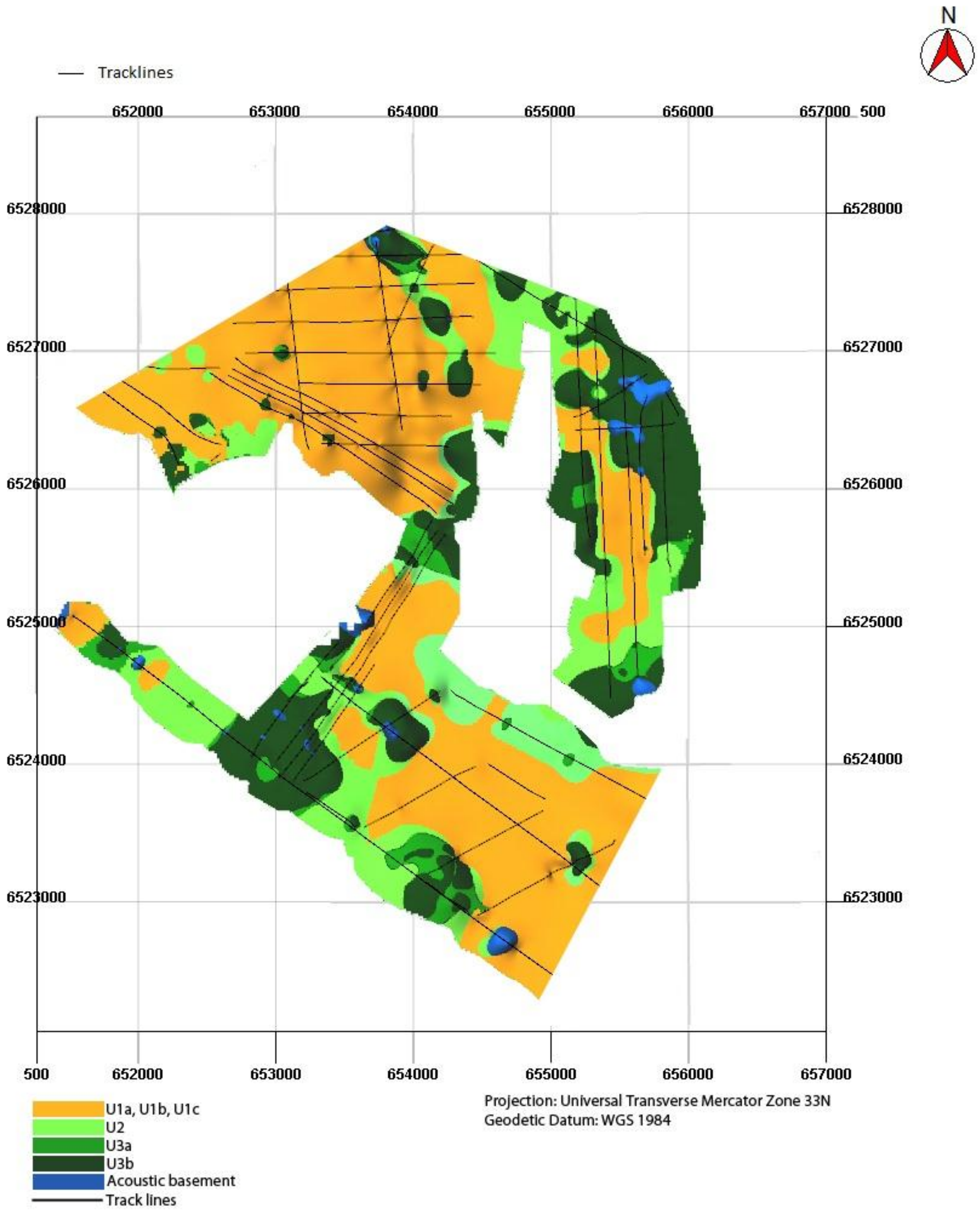

Figure 22: Sedimentological seafloor map. Each color represents an area where the unit is exposed at the seafloor. The map is based on a gridded result and the areas between the tracklines are therefore only a prognosis.

5.1.1 Glacial clay color transition

The color transition from brown to grey glacial clay is a frequently discussed topic in studies of the development of the Baltic Sea. Andrén (1999, 2002) presents a thorough analysis of the differences between the two colors and also dates the transition. Basically the brown glacial clay is older and has a different chemical and physical composition than the younger grey glacial clay.

In the descriptions of the Askö samples containing glacial clay, a difference in color from brown to grey is noted. It also seems to be related to the upper parts of U3. During this project, some effort was put into correlating the color transition in the cores with a reflector in the subbottom profile, especially the reflector separating U3a and U3b. However no tendency towards either color in each unit could be noted, the reasons for this can be several. The most obvious reason is that the color transition is represented by a less prominent reflector, then most likely within U3b, or that it is not represented at all. Other reasons could be related to the collection and interpretation of the data. Since the main purpose of the descriptions of the cores was educational it was performed by several people at different times. The perception of a tint can be quite individual and such circumstances would require some kind of standardized color description, which was not available on at least one occasion of interpretation. Another reason is the interpretation of the units in the seismic stratigraphy where it can be partly difficult to decide which of the U3 subunits are actually being sampled. This difficulty lies in the nature of the seismo-acoustic method as the signatures of sediments differ depending on its yielded resolution which in its turn depends on its depth. The boat, from which the samplings have been carried out, can also drift some meters from the time the position is noted and the sampling is performed.

5.1.2 Chronology of the sediment units

Since U3b is interpreted as distally deposited glacial clay, its portions closest to the acoustic basement can most likely be dated proximate to the time after the Younger Dryas ice regression. Accepting the ice sheet development presented by Brunnberg (1995), the area was just about covered by ice at the Younger Dryas ice maximum at 11500 clay varve years BP, which corresponds to 12260 cal. y BP according to Andrén (1999, 2002). This means that the basal parts of the glacial clay were deposited sometime after 12260 cal. y BP. How close in time depends on at which rate the melting occurred and when the melting started. Deciding the rate of melting across the project area is difficult since the ice sheet was probably not regressing at a steady pace. On the other hand, since the area is assumed to have been close to the ice rim of the Younger Dryas glacial maximum, the start of the melting may be estimated with a reasonable accuracy. Andrén (1999, 2002) dates the first occurrence of ice-rafted-debris to 11710 cal. y BP which may be used as an indicator of ice regression and also as a pointer to the earliest date of the lower portions of U3b. A method of dating the upper parts of the glacial clay without knowing the sedimentation rate is to determine the position in the subbottom profiles of the brown to grey color transition found in glacial clays in the Baltic. Andrén et al. (1999, 2002) dates this transition to around 11500 cal. y BP. Since there are no clear indication of a correlation between a reflector or unit and the brown to grey color transition, the position for the color change is still unclear.

There are three more likely alternatives for the marker of the color transition:

- The transition is marked by the prominent reflector separating U3b and U3a.
- U3a contains both types of clay and the acoustic reflector separating U3b and U3a is a marker to the final drainage of the Baltic Ice Lake. Andrén (1999, 2002) dates this drainage event to precede the color transition by merely a few decades.
- The position is marked by a less prominent reflector, most likely located within U3b.

Another indication that the U3a deposits can be related to events in Younger Dryas is found in a seismic investigation of the Gulf of Riga presented by Tsyrulnikov et al. (2012). As for seismo-acoustic signatures, the recordings presented from the Riga Bay show many similarities with the Askö area (Figure 23). However none of the units is similar to U3a. Since the Gulf of Riga was ice free during Younger Dryas (Donner, 2010) and the Askö region was not. U3a could be exclusively tied to this event.

Accepting that the lower boundary of U3a represents either the Final drainage of the Baltic Ice Lake or the color change from brown to grey (11560 /11525 cal. y BP (Andrén 1999, 2002)), its upper boundary can then be assumed to represent the Younger Dryas/Preboreal transition. This would date this reflector to 11 525 cal. y BP (Andrén 1999, 2002). The lack of laminations and the low organic content of U2 indicates that it was deposited during the Baltic Sea stages Yoldia Sea- Ancylus lake (Björck, 2008). This places the upper boundary of U2 at the onset of the Littorina Sea /Baltic Sea, around 8500 cal. y BP, whose sediments have a higher organic content (Björck, 2008).

Seismo acoustic Unit	Lithostratigrafic unit	Interpretation	Stage Baltic sea
U1a	Mud/ooze	Recently deposited	Littorina Sea / Baltic Sea
U1b	Mud/ooze	Recently deposited	Littorina Sea / Baltic Sea
U1c	n/a	Recently deposited	Littorina Sea / Baltic Sea
U2	Clay	Postglacial	Yoldia Sea – Ancylus Lake
U3a	Laminated clay	Glacial clay	Baltic ice lake
U3b	Laminated clay	Glacial clay	Baltic ice lake

Table 2: Interpretations and depositional sequence of units. Correlations to Baltic Sea stage as described by Björck (2008)

5.1.3 Bathymetry

When analyzing the grids and seafloor maps over the area and connecting them with the other information available, one formation stands out which could be a remnant from the glacial readvance and regression. This formation is the deep underwater gully that forms Fifångsdjupet and runs between Kråmö and Oxnö and is well aligned with the glaciofluvial sediments on the southeastern part of Askö. This could be interpreted as formed by a sub-glacial meltwater channel. In comparison to the location Sibofjärden, located about 22 km west of the present area, near Hånömogen, from where glaciofluvial deposits are described by Persson (1983). The morphology is similar except that the gully has been cut off, probably due to glacisostatic rebound. Thus, Sibofjärden is now a lake with a maximum depth of 10m (Salonsaari 2009). The present area also has many bathymetric similarities with Torö, another glaciofluvial deposit along the Middle Swedish ice marginal zone (Jakobsson, 1995). The Torö area contains large amounts of glaciofluvial sediments deposited at the front of a larger bathymetric depression.

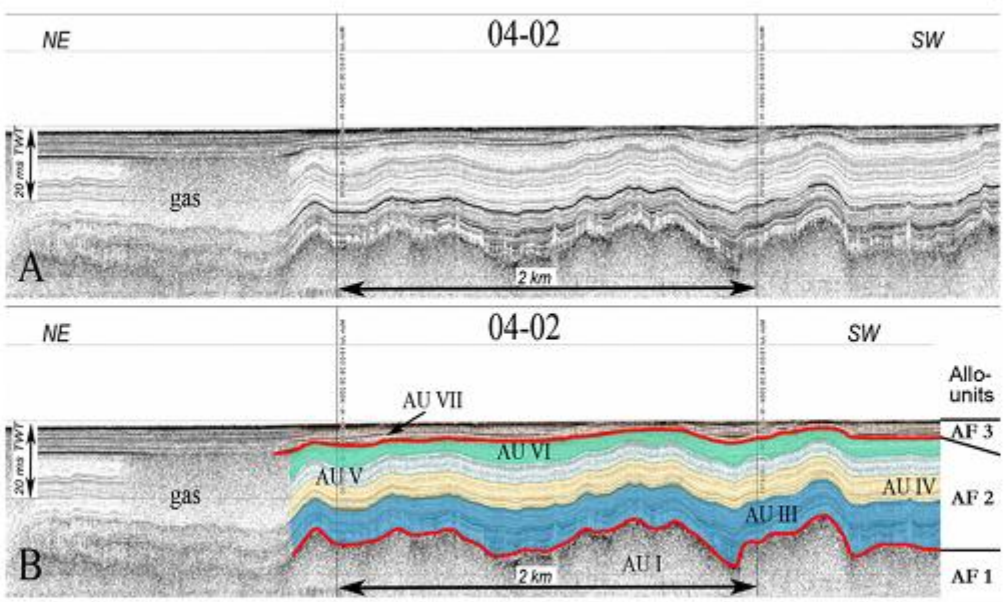

Figure 23: Acoustic profile with interpretation from Gulf of Riga (Tsyrulnikov et al. 2012). AUIII & AU IV is interpreted as deposited during BIL. AU V during Yoldia Sea. AU VI during Acylus Lake. AU VII during Litorina Sea/Post-Litorina (Tsyrulnikov et al. 2012). No unit has been interpreted as deposited during Younger Dryas. Comparing to Acoustic profiles from the Askö region, a signature resembling U3a is not represented.

5.2 Transport, Erosion and deposition

The interpretation of the ongoing erosion of sediments in the Askö area is based on the occurrence of recent sedimentation in the constructed grids. Where no recent sedimentation is found it is assumed that there is either ongoing erosion of the seafloor, or that the recent sediment layer is very thin because of continuous transport of deposited sediments.

The left map in Figure 24 illustrates areas where recently deposited sediments are present. Unmarked areas are void of recent sediments. Most of the areas that that are void of recent sedimentation are located at depths which should be out of reach of wave erosion. Consequently, the ongoing erosion is caused by current activity. Also the areas between Oxnö and Korpen and south of Stora Tallholmen (Figure 24 right), which have depths of 30-40 m and should be well out of reach from regular wave erosion, show indications of ongoing erosion and transport. This is probably caused by currents, along the marked parts in Figure 24 right, and further north through the shallower area past the islands Tvillingarna and towards the lighthouse on Svarthäll. Indications of the current direction are shown in Figure 26. The profile in the figure illustrates how the water depth increases relatively abruptly northwest of a knoll and that very young sediments are deposited there. This suggests a northeasterly current direction as it enters the project area and then deviates to the north between Oxnö and Korpen following the shallower parts in between Tvillingarna and Svarthäll. The depositional pattern in Figure 24 shows that these currents are probably the main transporter of the recent sediments deposited in the deeper parts of Fifångsdjupet. The absence of larger deposits in the 40 m deep depression between Oxnö and Korpen also suggests that a current strong enough to carry most of the sediments through is at work. The suggested current direction also conforms well with currents induced by air pressure differences in the Baltic, which would enter the area from the outer waters in the southeast, during low pressure in the west while high pressure in the eastern Baltic proper (SMHI, Lufttryck och Havsvattenstånd 2009).

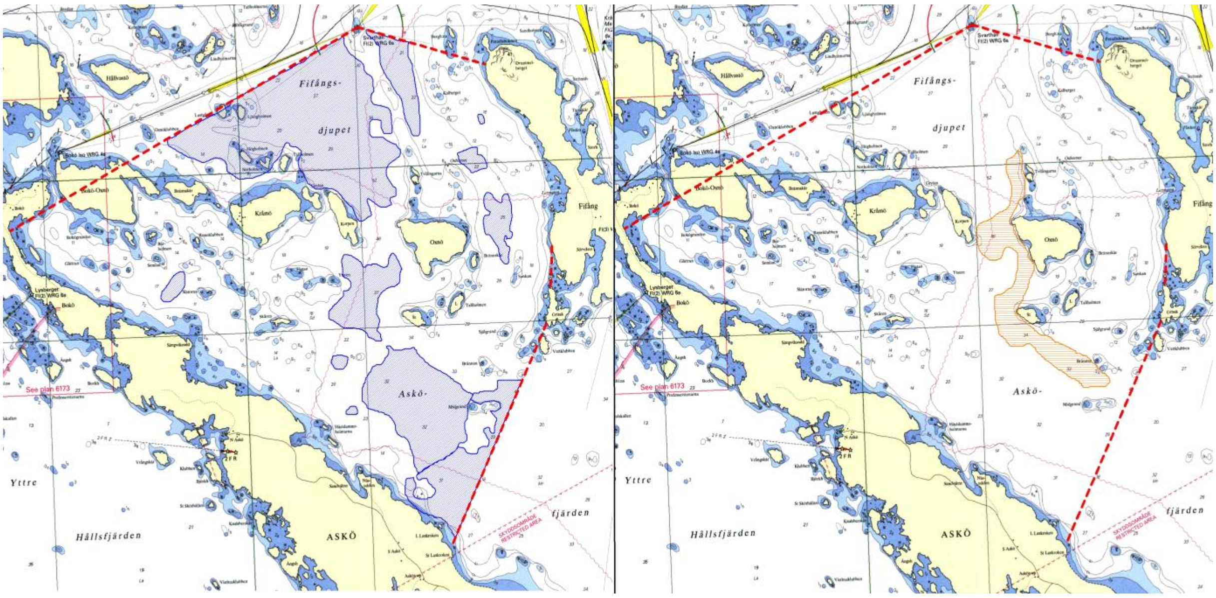

Figure 24: Left: The blue fields mark the areas of deposition and are based on the Isopach of U1 (Fig. 6). Right: The orange fields represent the deep seafloor erosion and marks areas with depths over 30 m and no or little recent sedimentation.

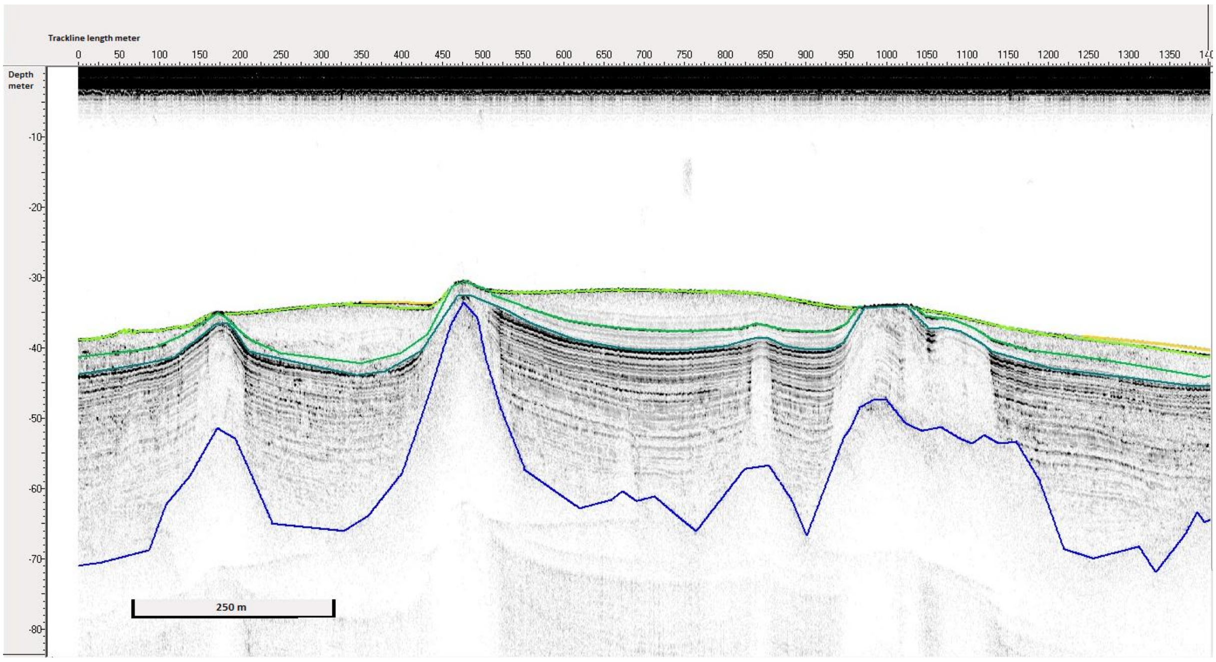

Figure 25: Chirp profile 09261214 with interpreted horizons. Illustrates an example of ongoing erosion and deposition.

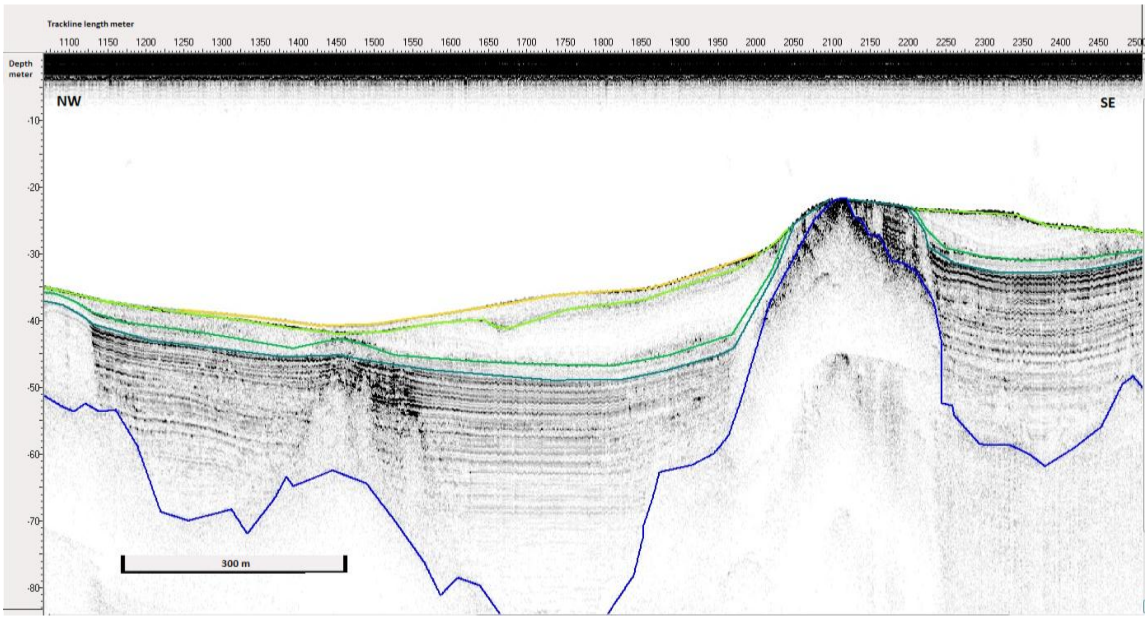

Figure 26: Chirp profile 9261214 with interpreted horizons. Illustrates recent deposits NW of knoll indicating direction of current.

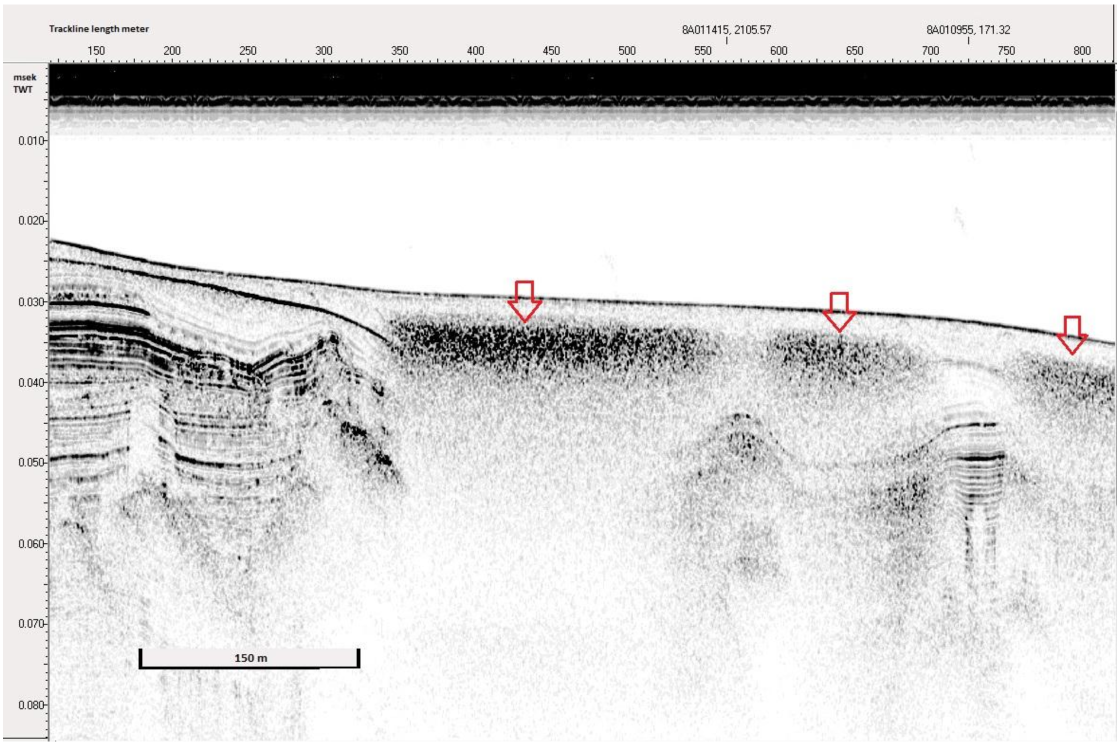

Figure 27: Chirp sonar profile along trackline 11311037. Illustrates a typical area where the acoustic signal is hindered from penetrating through the top sediment (marked with red arrows).

5.3 Gas accumulations and pockmarks

Gas charged sediments are widely spread around Askö. The gas-rich areas everywhere conform to postglacial surface sediments that are rich in mud. The origin of the gas in the Askö area is due to the normal biogenic processes in the mud, although minor contributions of thermogenic gas cannot be ruled out. No pockmarks in the seafloor have been observed in the present area (personal communication, Tom Flodén 2012), which may indicate that the gas production is only moderate with low or almost negligible contribution of thermogenic gas. A high production of gas in the mud is often observed along tectonic lineaments where there is a contribution of thermogenic gas from deep in the bedrock (Söderberg & Flodén 1989). These high production areas are often marked by pockmarks in the seafloor.

5.4 Ground water related structures

Söderberg and Flodén (1997) observed several large pockmark-like structures developed in the glacial clay at Sundsbådarna located roughly 5 km SE of the presently investigated area northeast of Askö. These structures were interpreted as being formed by groundwater outflow. Söderberg and Flodén (1997) further mention observations of groundwater outflows through a top layer of mud at Vettershaga, in the northern part of the Stockholm archipelago. Similar outflows of groundwater in mud areas are occasionally found all across the archipelago area, often forming positive seafloor structures, so called “mud volcanoes”.

In the Askö area, both southeast of Askö and within the present area northeast of the island, there occur terrace-like bedforms in glacial clay (Söderberg & Flodén 1997; personal communication, Tom Flodén 2013). These terraces often occur as several “steps” along the slopes to deeper water. They are provisionally interpreted as formed by groundwater outflow along layers of somewhat coarser materials in the glacial clay in a similar manner as for the structures at Sundsbådarna, described in Söderberg & Flodén 1997.

The relationships between biogenic gas, thermogenic gas and groundwater outflows in the archipelago are still largely unknown. However, there is reason to make a connection between the Askö and the Vättershaga areas as they are both located along major lineaments in the Svecofennian bedrock, Södertäljeleden for Askö and Furusundsleden for Vettershaga. Thus, there is a slight possibility for thermogenic gas deriving from tectonic lineaments in the Askö area as well.

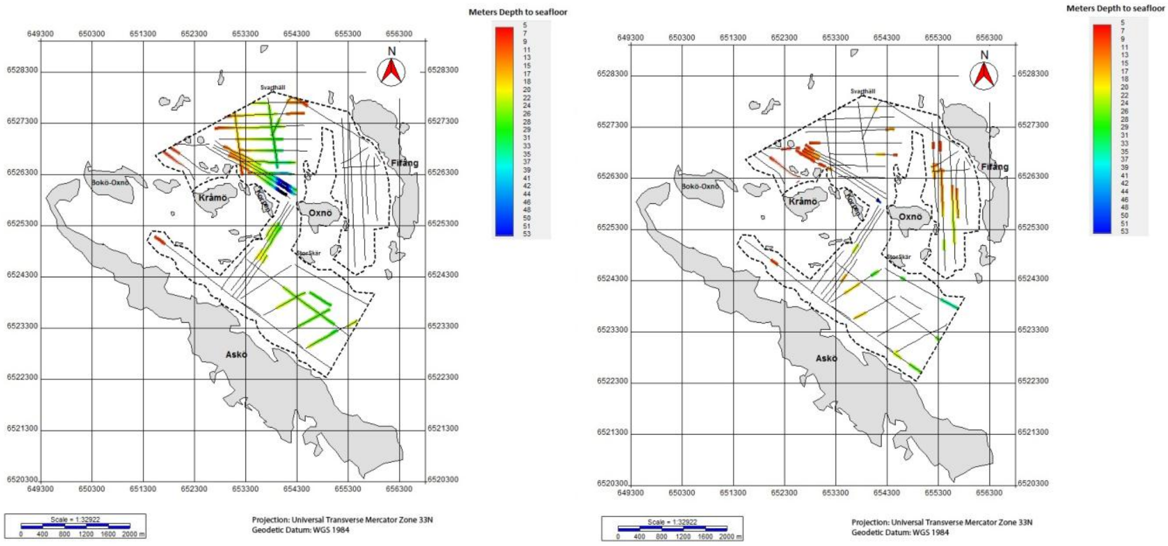

Figure 28. Locations where recent sediments have been interpreted along the tracklines. Left map shows recent sediments containing gas. Right map shows recent sediments without signs of gas.

6 Conclusions

This study presents a marine high resolution seismo-acoustic study of a 12 km^2 large area just north of the island of Askö in Trosa archipelago. The main focus points are to geologically interpret the data, investigate possible areas of erosion and its causes, and to map areas of gas accumulation.
The interpretation and presentation was done using the seismic and geological interpretation software SMT kingdom.

From the results the following conclusions could be made:

- In total of 3 main units with corresponding subunits where distinguished, U3, U2 and U1. The correlation between the seismo-acoustic data and core descriptions show deposits of glacial clay at the bottom, overlain by postglacial clay and recent deposited gas rich mud and clay. U3 is the oldest unit, deposited after the Younger Dryas ice maximum around 11710 cal. y BP. The reflector between its two sub units, U3a and U3b, possibly reflect the drainage of the Baltic Ice Lake, which would date the U3a lower boundary to around 11 560 cal. y BP and its upper boundary to the Younger Dryas/preboreal transition around 11525 cal. y BP. U2 has most likely been deposited during the Baltic Sea stages Yoldia Sea- Ancylus lake, dating its upper boundary to the onset of the Littorina Sea /Baltic sea, around 8500 cal. y BP. U1 with its 3 subunits, U1a, U1b and U1c are deposited during the present stage of the Baltic Sea.

- The interpretation of the core samples shows a brown to grey color difference in the glacial clay deposits. This color transition has been identified in previous investigations within nearby areas and has been dated to around 11500 cal. y BP, which is relatively close in time to the drainage of the BIL. It was further investigated during this study whether this noted color difference could be correlated to the reflector separating the two sub units U3a and U3b but no solid evidence could be seen. Investigations in the Gulf of Riga may, however possibly link the U3a reflector to events triggered during the late Younger Dryas. This due to the lack of observations of a similar unit to U3a in the Gulf of Riga investigation. Since this project was not focused to answer this particular question, future investigations are apt to come up with a satisfactory answer.

- The grids constructed over the recent sedimentation show several areas that undergo erosion. Generally, the area is estimated not to be seriously affected by wave erosion but rather erosion from bottom currents. The deepest parts of the area, measuring 30-40 m in depth, show obvious signs of erosion in the sediments which consequently is most likely caused by current activity induced by air pressure differences over the Baltic and the Swedish inland. The direction of the currents can possibly be determined by the depositional pattern of the sediments in this area. Suggesting an SE to NW current direction.

- Gas induced recent sediments are quite common throughout the area, even more common than recent sediments without signs of gas, as can be seen in Figure 27. Two alternatives for the origin of similar gas findings have been presented: biogenic (most common) produced by bacterial activity, and thermogenic, derived from deep within the earth's crust and escaping through tectonic lineaments. Lack of observations of pockmarks in the area and the dominating gas occurrence in connection with mud rich sediments suggest the majority of the gas produced in the area is of a biogenic origin. But further geochemical investigations are needed before a thermogenic origin can be excluded.

The quality of the interpretation and the availability of data from the core samples vary, consequently this have an effect on the certainties of the geological interpretation in this report. However, the tendencies observed in the data still raises interesting questions to be further investigated.

7 Acknowledgements

I want to thank my supervisor Richard Gyllencreutz for all his support and guidance during the project. I would also extend my gratitude to Tom Flodén and Martin Jakobsson for their advice and expert opinions.

8 References

Andrén, T., Björck, J., Johnsen, S., 1999: Correlation of Swedish glacial varves with the Greenland (GRIP) oxygen isotope record. Journal of Quaternary Science 14, 361-371.

Andrén, T., Lindeberg, G., Andrén, E., 2002: Evidence of the final drainage of the Baltic IceLake and the brackish phase of the Yoldia Sea in glacial varves from the Baltic Sea. Boreas , Vol. 31: 226 –238. Oslo. ISSN 0300-9483.

Björck, S., 2008: The late Quaternary development of the Baltic Sea. In The BACC Authors Team (eds), Assessment of climate change for the Baltic Sea Basin. Springer–Verlag, Berlin–Heidelberg, pp 398–407.

Boggs, S., 2006: Principles of sedimentology and stratigraphy, 4th ed. Pearson Education, London. 662 pp.

Brunnberg, L., 1995: Clay-varve chronology and deglaciation during the Younger Dryas and preboreal in the easternmost part of the Middle Swedish Ice Marginal Zone. Quaternaria. Serie A No 2. PhD Dissertation, Stockholm University, Stockholm, Sweden.

Donner, J., 2011: The Younger Dryas age of the Salpausselkä end moraines in Finland. Bulletin of the Geological So-ciety of Finland 82. pp 69–80.

Fleischer, P., Orsi, T., Richardson, M., Anderson, A., 2001: Distribution of free gas in marine sediments: a global overview. Geo-Marine Letters. pp 103-122.

Flodén, T., 2012: Bathymetry of the area NE of Askö Island, Södertörn. Unpublished work material.

Flodén, T., Söderberg, P., 1994: Shallow gas traps and gas migration models in crystalline bedrock areas offshore Sweden. Baltica, Vol. 8, pp.50-56. Vilnius. ISBN 9986-615-01-1

Floodgate, G., Judd, A., 1992: The origins of shallow gas. Continental Shelf Research. Vol 12, No. 10. pp 1145-1156.

Fredén, C. (red.), 2009: Berg och jord. Sveriges Nationalatlas, tredje upplagan andra tryckningen, SNA förlag. Stockholm, Sweden. 208 pp.
Hell, B., Jakobsson, M., 2011: Gridding heterogeneous bathymetric data sets with stacked continuous curvature splines in tension. Marine Geophysical Research, 32(4), 493–501, DOI:10.1007/s11001-011-9141-1.
Hovland, M., Judd, A., 1988: Seabed pockmarks and seepages—Impact on Geology, Biology and the Marine Environment. Graham and Trotman. Oxford. 293 pp
Hyttinen, O., Kotilainen, A., Salonen, V.-P., 2011: Acoustic evidence of a Baltic Ice Lake drainage debrite in the northern Baltic Sea. Marine Geology 284. pp 139–148.
Håkanson L., Bryhn A., 2008: Eutrophication in the Baltic Sea: Present Situation, Nutrient Transport Processes, Remedial Strategies - Chapter 2: Basic information on the Baltic Sea. Environmental Science and Engineering, Springer, Berlin. ISBN: 978-3-540-70909-1 (Online).
Jakobsson, M., 1995: Glacial and postglacial development of the Ören deposit south-west of Torö, southern Stockholm Archipelago, Sweden. Master thesis. Stockholm university Department of quarternary research, Department of geology and geochemistry.
Jonsson, P., Persson, J., Holmberg, P., 2003: Skärgårdens bottnar. Report 5212, Swedish Enviromental Protection Agency. (In Swedish with English summary).
Judd, A., Hovland, M., 1992: The evidence of shallow gas in marine sediments. Continental Shelf Research 12. pp 1081–1095.
Laier, T., Kuijpers, A., Dennegård, B., Heier-Nielsen, S., 1996: Origin of shallow gas in Skagerrak and Kattegat - evidence from stable isotopic analyses and radiocarbon dating. NGU Bulletin, 430, pp 129-136.
Lokrantz, H., Sohlenius, G., 2006: Ice marginal fluctuations during the Weichselian glaciation in Fennoscandia, a literature review, Tech. Rep. TR-06-36, Swedish Nuclear Fuel and Waste Managment Co. (SKB). Stockholm, Sweden.
Lundqvist, J., 1987: Glaciodynamics of the Younger Dryas Marginal Zone in Scandinavia. Implications of a revised glaciation model. Geogr. Ann, 69A (2). pp 305-319.
Lundqvist, J., 1995: The Younger Dryas ice-marginal zone in Sweden. Quaternary International, Vol. 28. pp 171-176.
Parkes, R., Crags, B., Fry, J., Herbert, R., Wimpenny, J., 1990: Bacterial biomass and activity in deep sediment layers from the Peru margin Philosophical Transactions of the Royal Society of London, A331. pp 139-153.
Persson, C., 1983: Glacial deposits and the central Swedish end moraine zone in eastern Sweden. In Ehlers, J. (ed.): Glacial Deposits in North-West Europe. Balkema, Rotterdam. pp 131-139.
Reading, H., and Levell, B., 1996: Controls on the sedimentary rock record. In: Reading, H.G. (Ed.), 1996. Sedimentary environments: processes, facies, and stratigraphy, 3rd ed. Blackwell Science, Oxford. 688 pp.
Salonsaari, J., 2009: Övergödda havsvikar och kustnära sjöar inom Norra Östersjöns vattendistrikt – redovisning av regeringsuppdrag. Länsstyrelsen i Västmanlands län. Rapport 2009:5. (In Swedish)
Schoch, S., LeBlanc, L., Mayer, L., 1989: Chirp subbottom profiler for quantitative sediment analysis. Geophysics 54. pp 445-450.
SMHI, Lufttryck och Havsvattenstånd, 2009: http://www.smhi.se/kunskapsbanken/oceanografi/lufttryck-och-havsvattenstand-1.3096
SMHI, Vindvågor, 2009: http://www.smhi.se/kunskapsbanken/oceanografi/vindvagor-1.1748
Smith, W., 1993: On the Accuracy of Digital BathymetricData. *Journal of Geophysical Research*, 98(B6). pp 9591–9603.
SMT Kingdom v.8.7.1 manual: Digital software manual. Available through www.ihs.com.
Söderberg, P., 1993: Marine geological investigations in the Åland Sea and the Stockholm Archipelago, Sweden – Seismic stratigaphy, tectonics and occurrences of gas related structures. Stockholm University, Department of Geology and Geochemistry, S-106 91. Stockholm, Sweden. ISBN 91 87786-07-9.

Söderberg, P., Flodén, T., 1989: Geofysiska och geokeimska undersökningar i anslutning till tektoniska linerament i Stockholms skärgård – undersökningar vid Vetterhaga och Stavsnäs, 1984 – 1988. *Vattenfall, Naturgas, Utveckling och Miljö U(G)1989/20*, 1-69, (In Swedish with English summary).

Söderberg, P., Flodén, T., 1992: Gas seepages, gas eruptions and degassing structures in the seafloor along the Strömma tectonic lineament in the crystalline Stockholm Archipelago, east Sweden.

Söderberg, P., Flodén, T., 1997: Stratabound submarine terraces and pockmarks – indicators of spring sapping in glacial clay, Stockholm Archipelago, Sweden. In Cato, I., Klingberg, F. (eds): Proceedings of the Fourth Marine Geological Conference – the Baltic, Uppsala 1995. Sveriges Geologiska Undersökning, Ser. Ca 86. pp 173-178. ISBN 91-7158-553-2.

Tsyrulnikov, A., Tuuling, I., Kalm, V., Hang, T., Flodén, T., 2012: Late Weichselian and Holocene seismo-stratigraphy and depositional history of the Gulf of Riga, NE Baltic Sea. Boreas, 10.1111/j.1502-3885.2012.00257.x. ISSN 0300-9483.

Appendix 1

A large part of the project included learning and working with the seismic and geological interpretation software SMT kingdom. At the time this project started this software was recently acquired by the institution and there was no real internal knowledge on how to operate the software. To facilitate future users of the software, all important steps and the workflow in which the data was imported, interpreted and finally, gridded is reported in this appendix.

Import process

1) Import the processed SEGy files with the multi import tool. Make sure all the necessary information from the files header is available.
2) See below.

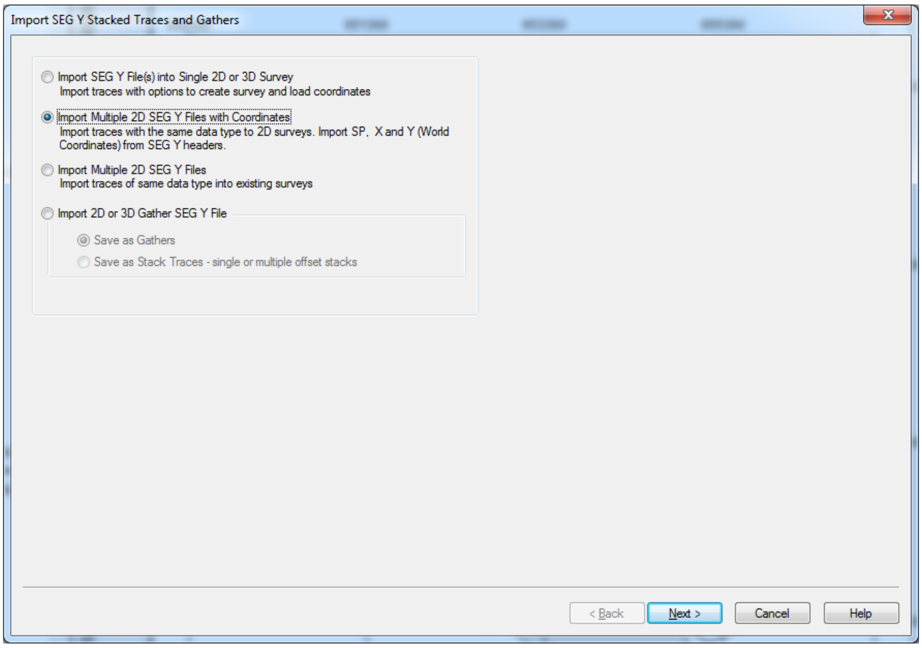

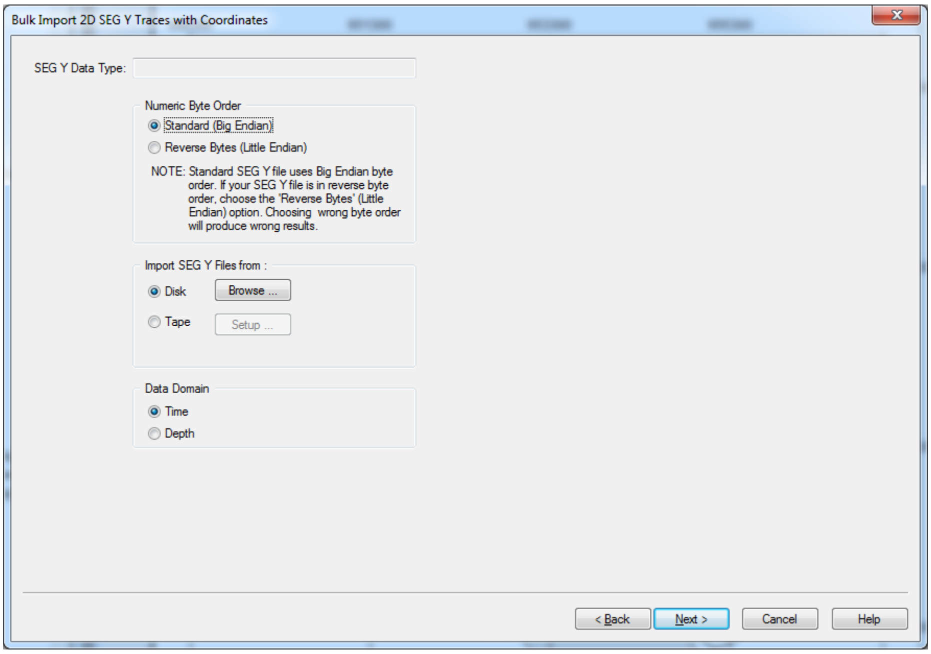

3) Select multiple segy files for the bulk import.

4) Specify Amplitude format

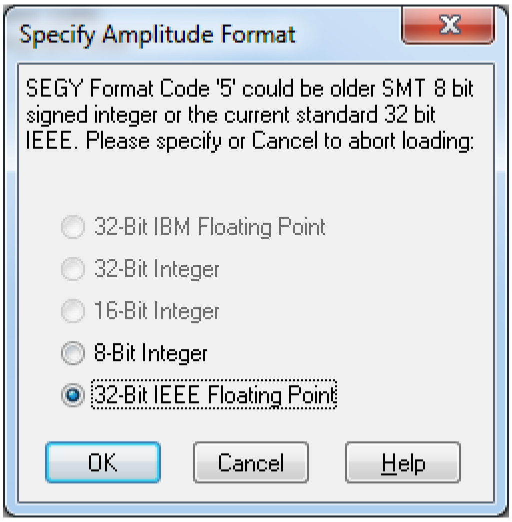

5)

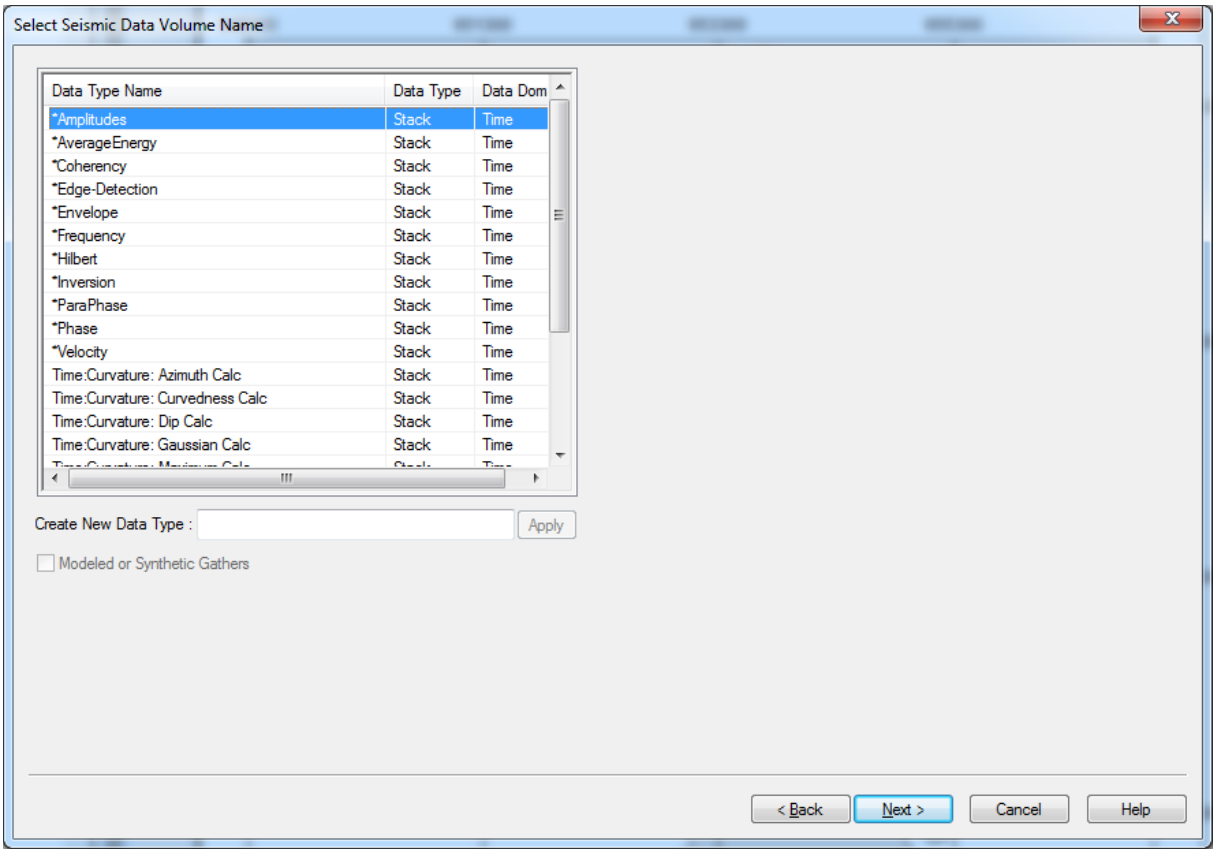

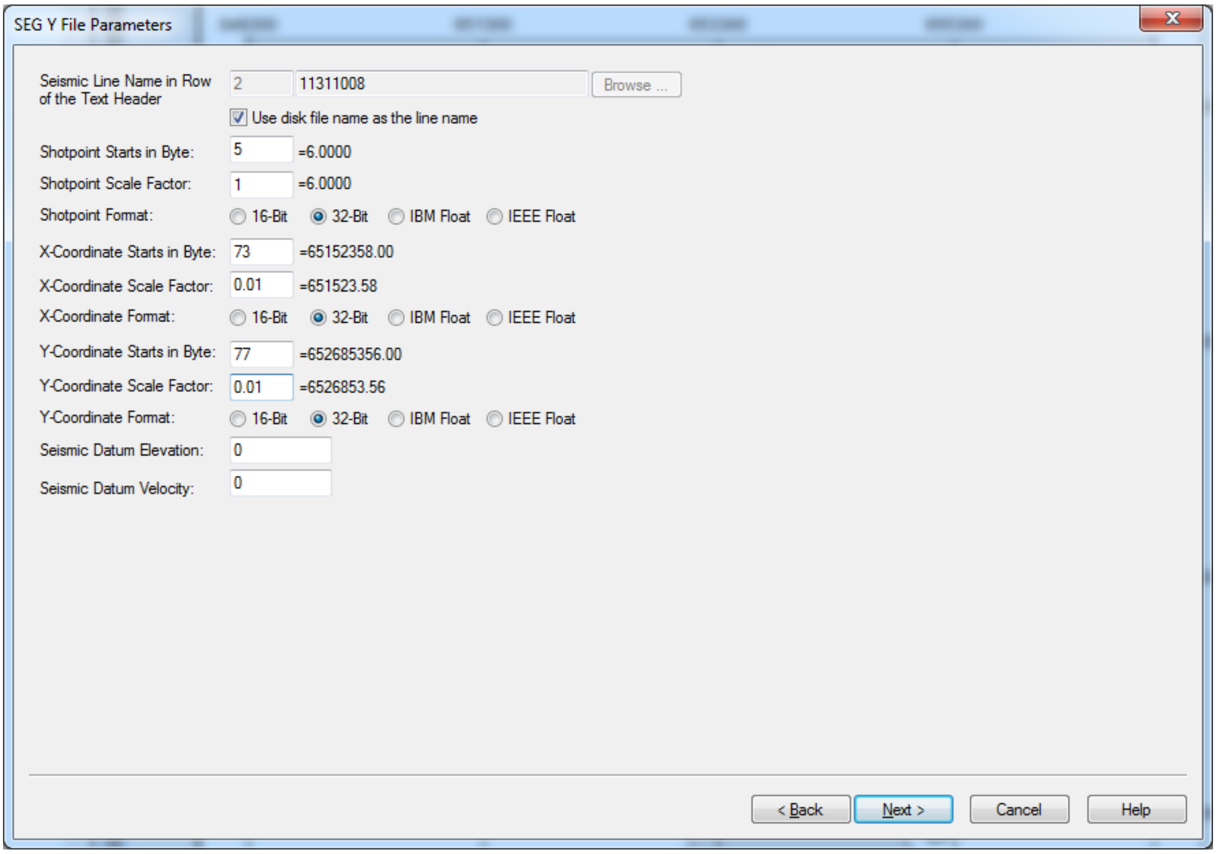
SEG Y File Parameters
Seismic Line Name in Row of the Text Header
2
11311008
Browse ...
Use disk file name as the line name
Shotpoint Starts in Byte: 5 =6.0000
Shotpoint Scale Factor: 1 =6.0000
Shotpoint Format: 16-Bit 32-Bit IBM Float IEEE Float
X-Coordinate Starts in Byte: 73 =65152358.00
X-Coordinate Scale Factor: 0.01 =651523.58
X-Coordinate Format: 16-Bit 32-Bit IBM Float IEEE Float
Y-Coordinate Starts in Byte: 77 =652685356.00
Y-Coordinate Scale Factor: 0.01 =6526853.56
Y-Coordinate Format: 16-Bit 32-Bit IBM Float IEEE Float
Seismic Datum Elevation: 0
Seismic Datum Velocity: 0
< Back
Next >
Cancel
Help

6)

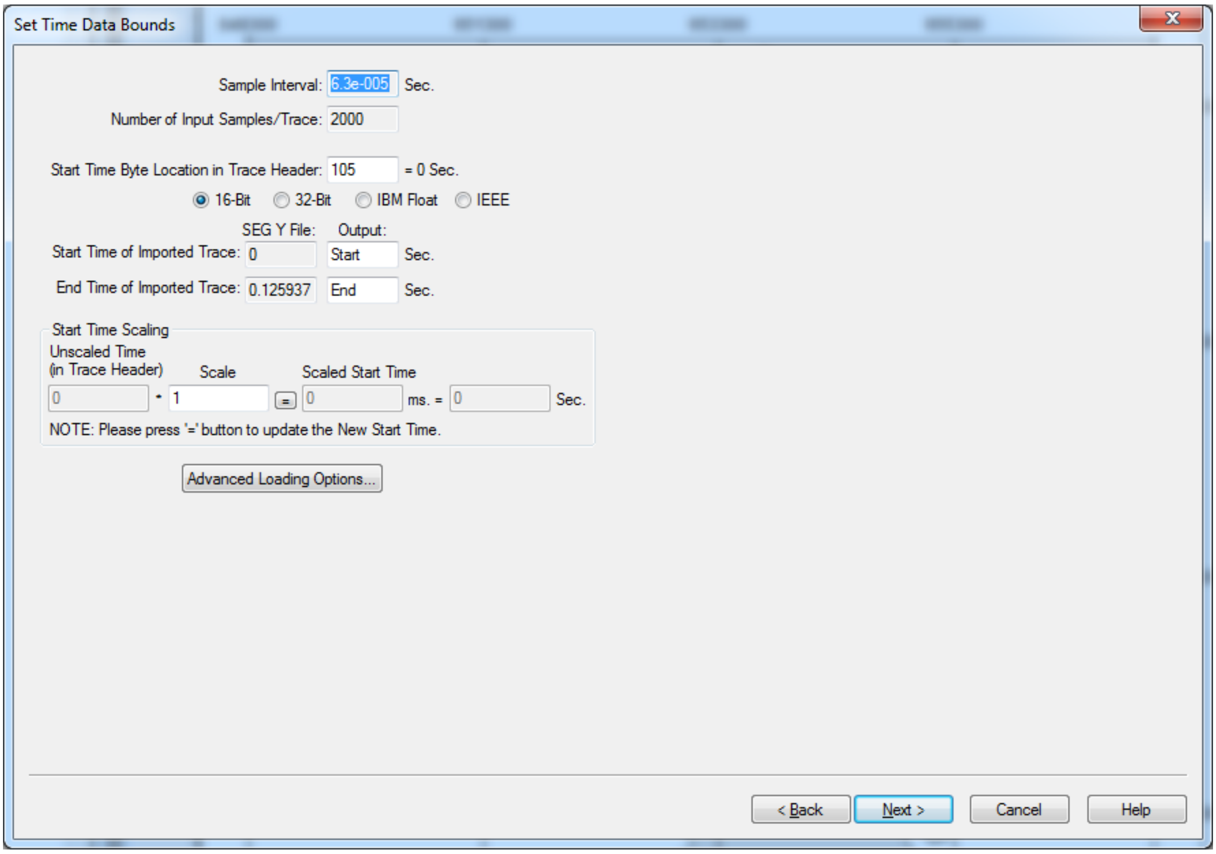
Set Time Data Bounds
Sample Interval: 6.3e-005 Sec.
Number of Input Samples/Trace: 2000
Start Time Byte Location in Trace Header: 105 = 0 Sec.
16-Bit 32-Bit IBM Float IEEE
SEG Y File: Output:
Start Time of Imported Trace: 0 Start Sec.
End Time of Imported Trace: 0.125937 End Sec.
Start Time Scaling
Unscaled Time (in Trace Header)
Scale
Scaled Start Time
0 * 1 = 0 ms. = 0 Sec.
NOTE: Please press '=' button to update the New Start Time.
Advanced Loading Options...
< Back
Next >
Cancel
Help

7)

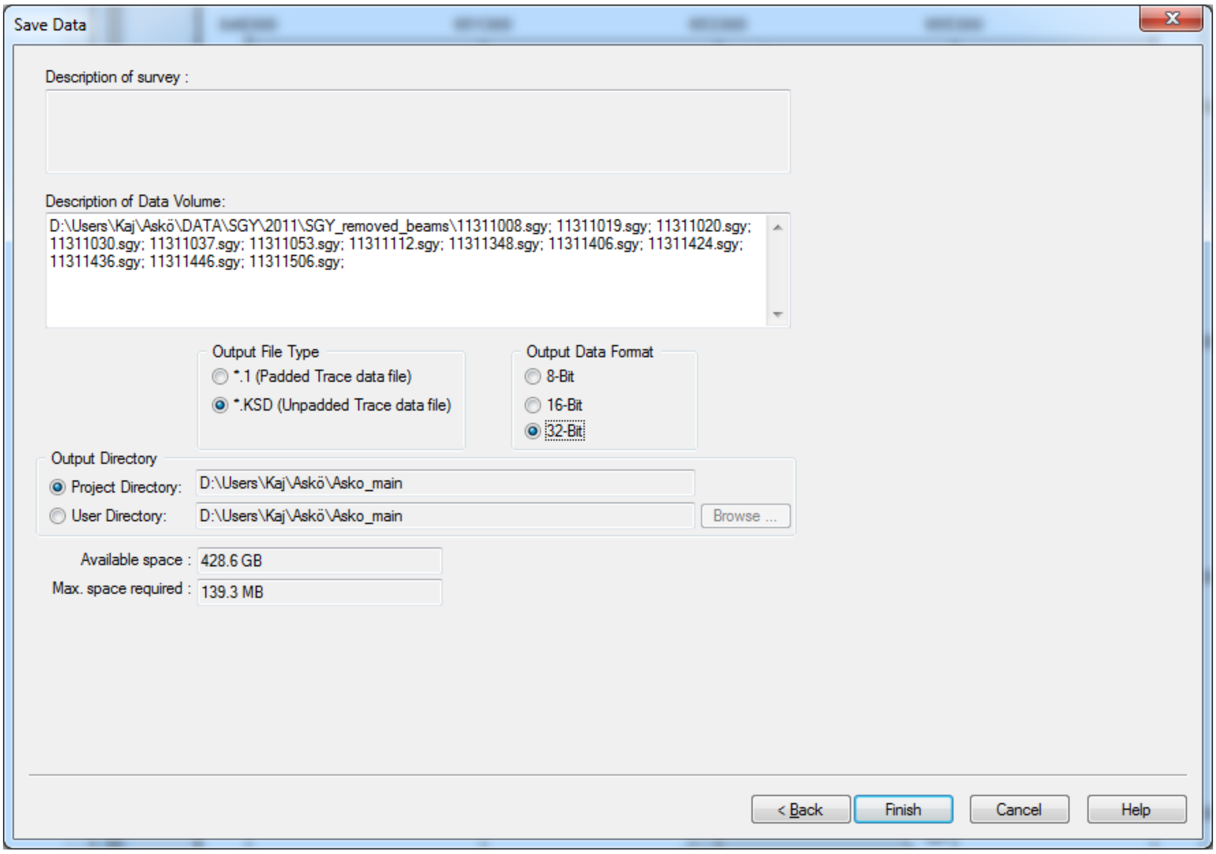

8)

9) Now the SEGy is imported and can be viewed in the project tree and the base map

Time -> depth conversion

1) To convert your data that where imported with the time domain selected to depth domain choose from the main menu Tools-> Trace calculations -> Time<> depth conversion
2) Select all surveys

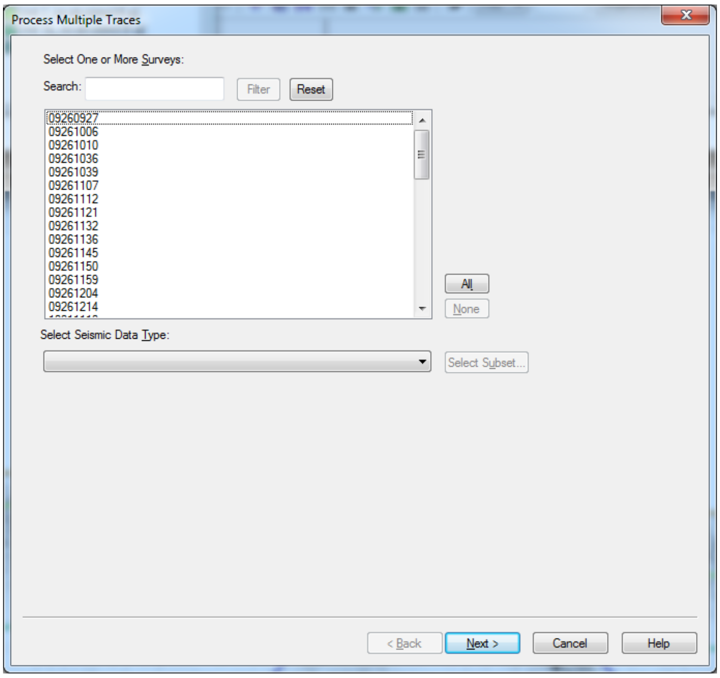

3) Select process

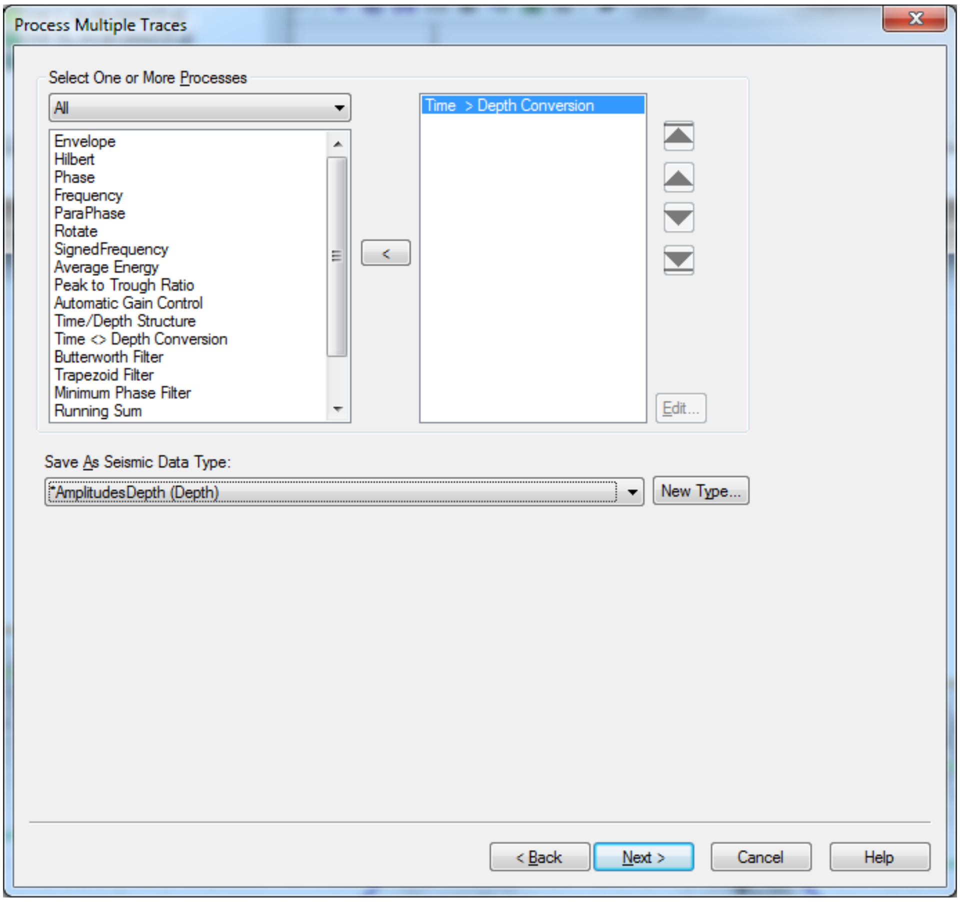

4) Select process, in this case a sound velocity of 1469 m/s were used

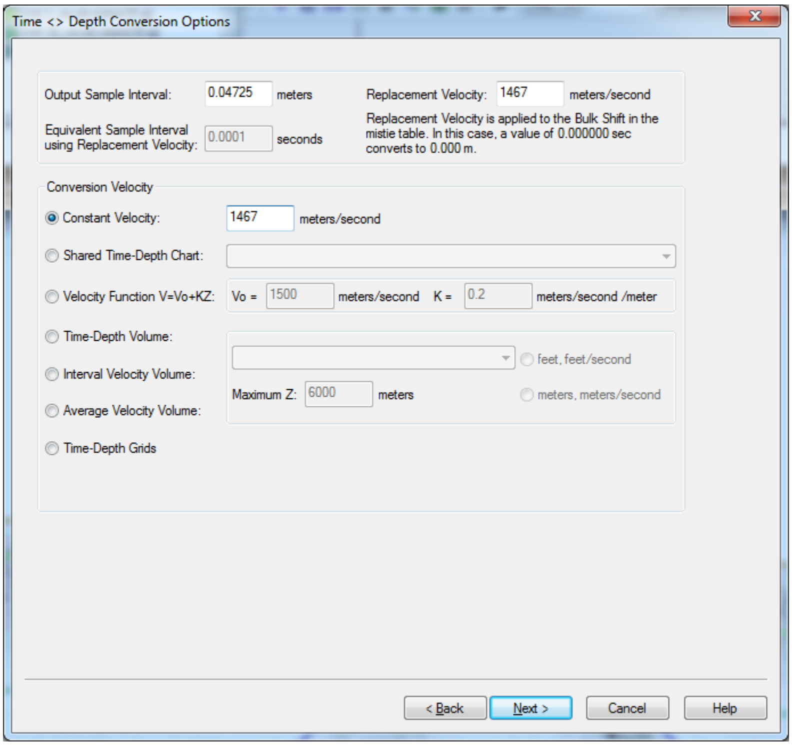

5) Press apply in next window and save to root of the project folder (Important)

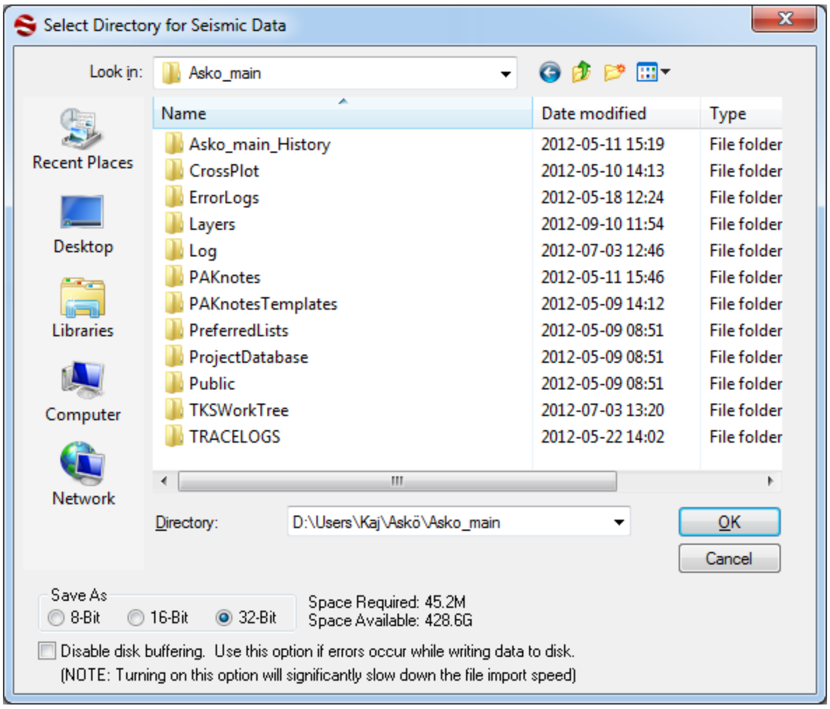

6) The data domain Amplitudes depth can now be selected in the seismic window

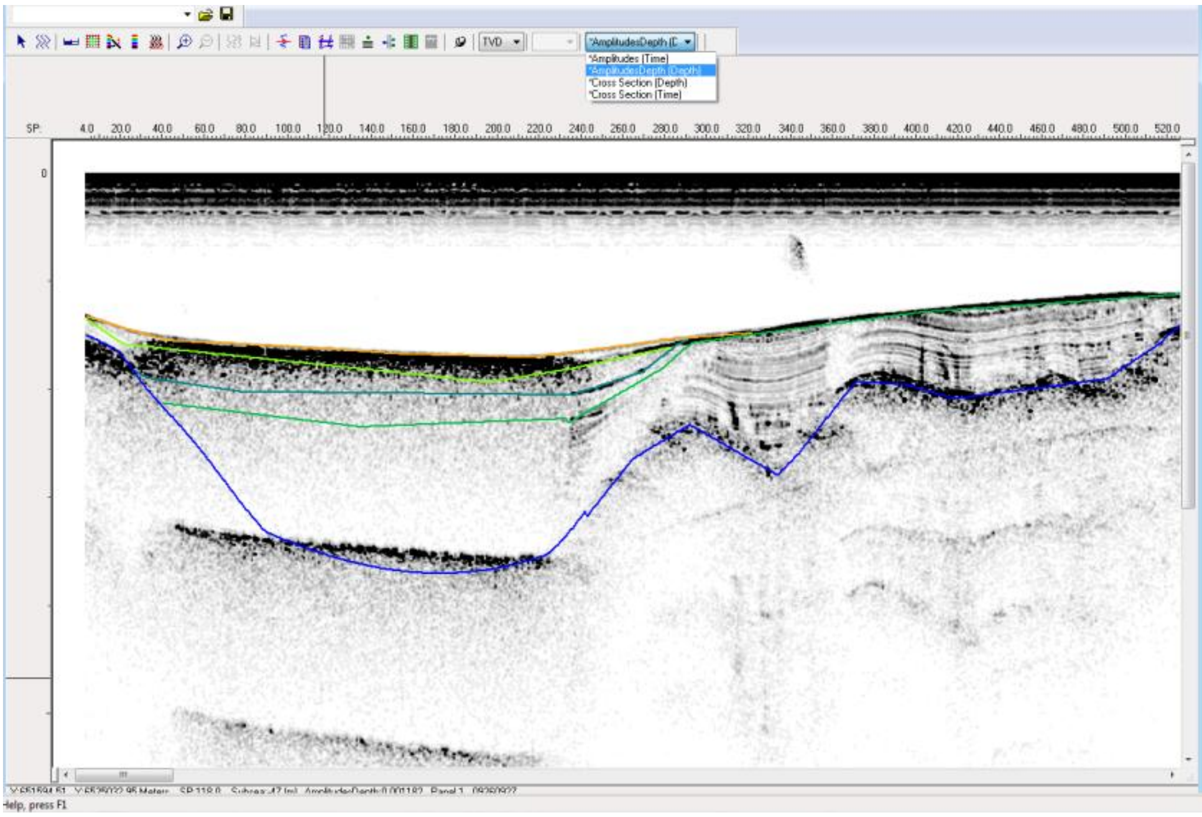

Horizon interpretation

1) Create your horizons under horizons in main menu-> horizon management -> Create
2) View your created horizons by selecting View-> toolbars->Horizons picking.
   You will need to have your created horizons activated in the project tree to be able to view them in the horizons picking window.

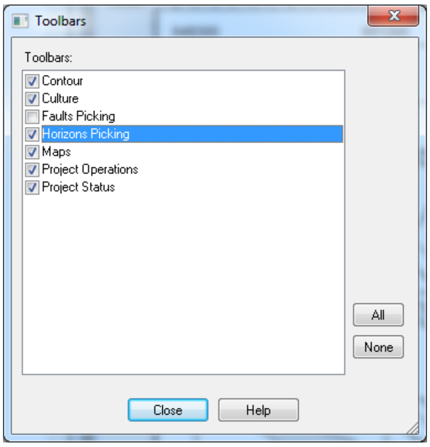

3) You can now start to digitize each horizon

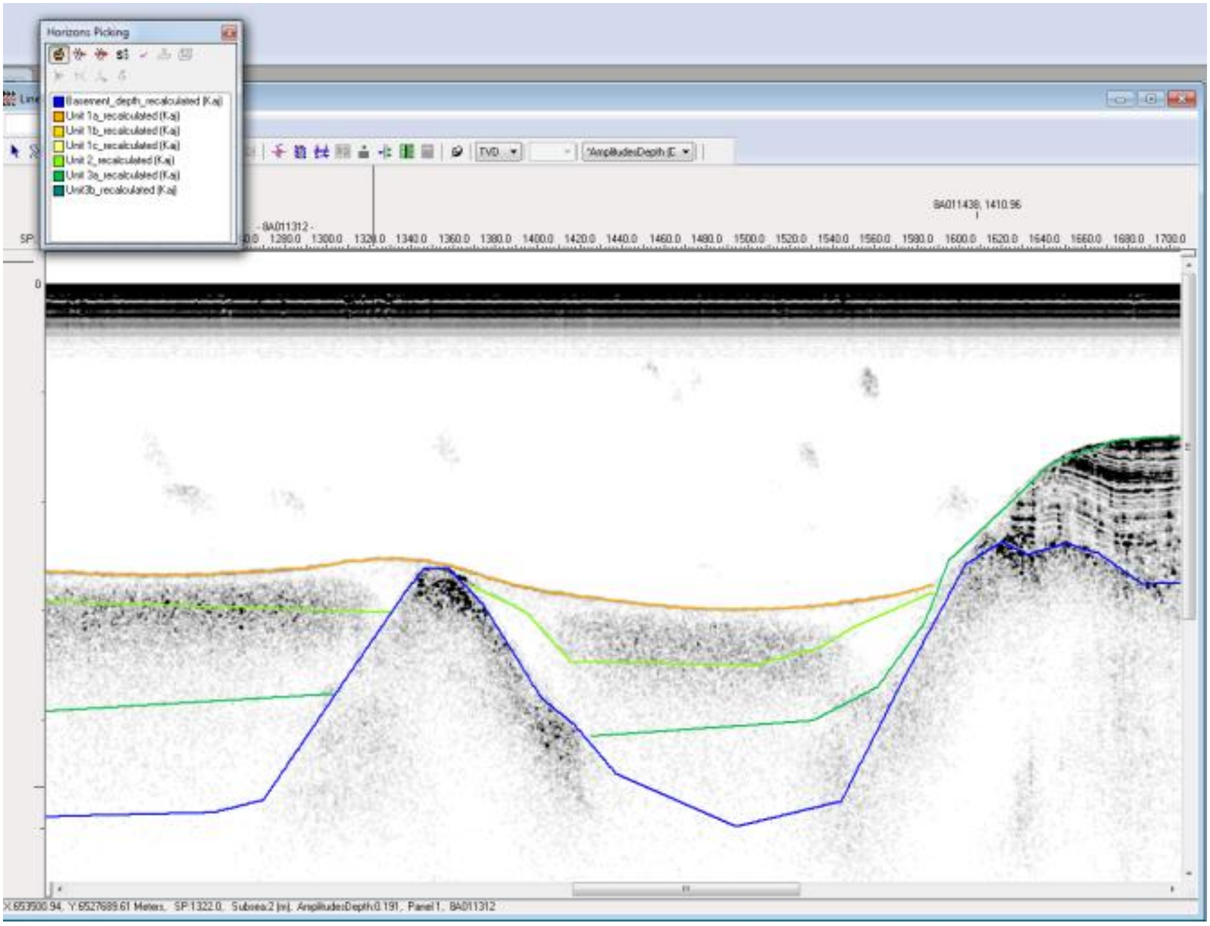

Grid horizons

1) When all wanted seismic reflectors have been digitized they can be gridded under main menu Grids->Create grids
   The used settings for the project shown below

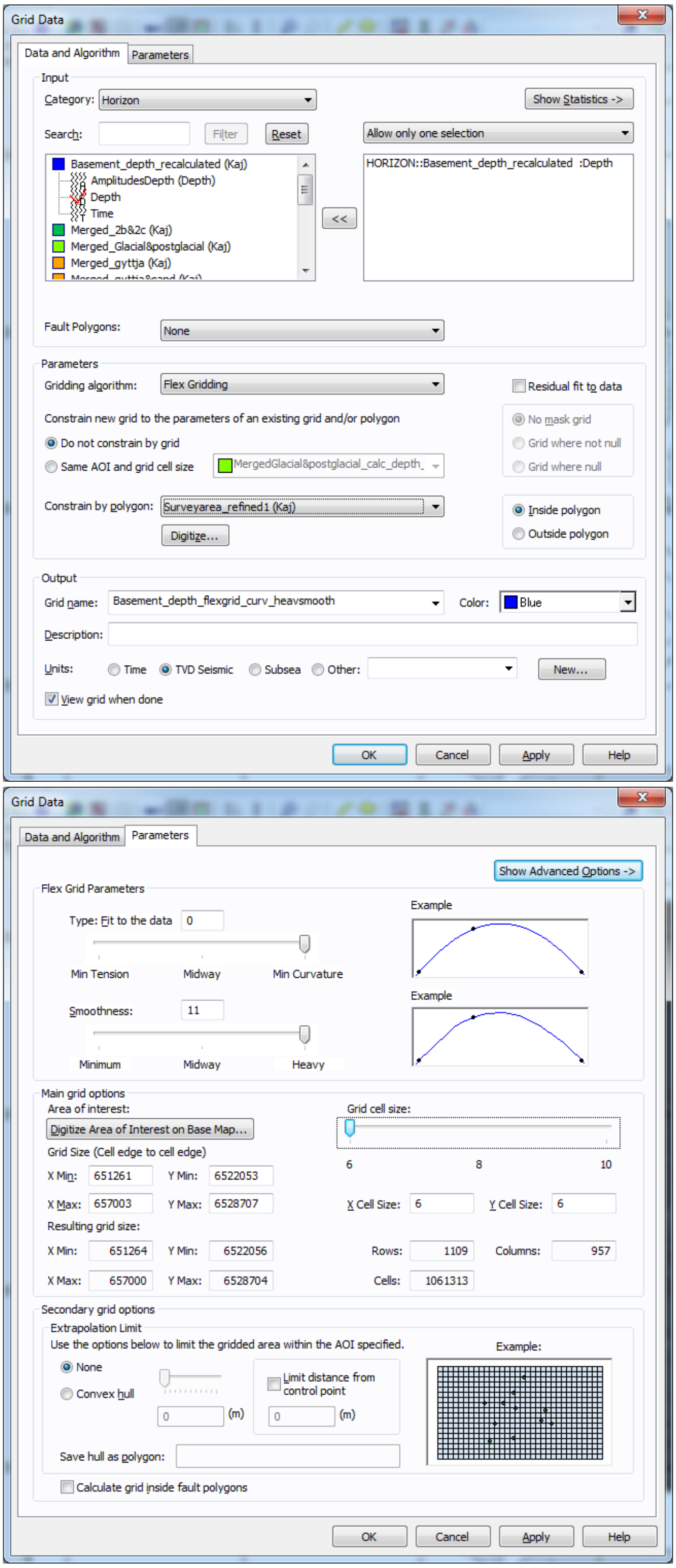

2)The grid is now created and can be viewed from the project tree.

Extended math calculator

Is accessed under main menu Tools-> calculators-> extended math

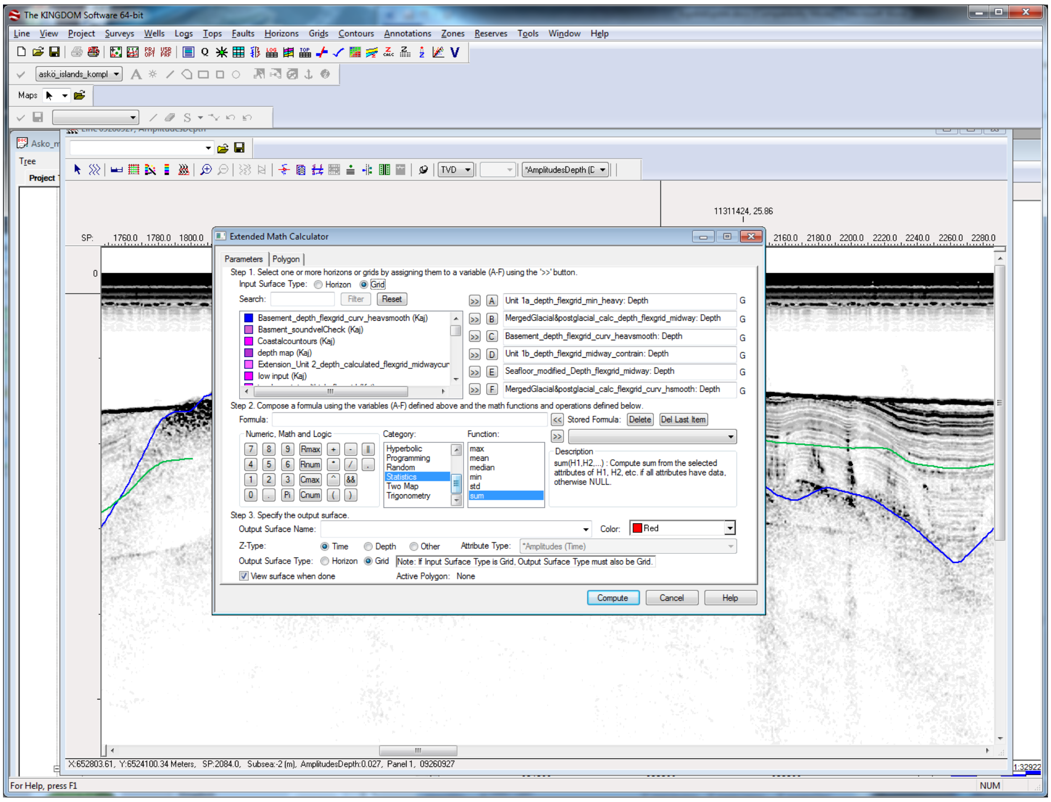

Isopach grid

The extended calculator was used to create the isopach grids.

1) To create an isopach grid the lower grid is subtracted from the overlying.
Formula: A-B
Total Sediment calculation: Acoustic basement subtracted by Seafloor
Recent sediment calculation: Merged_U3a&U3b&U2 subtracted by Merged_U1a&U1b&U1c
Glacial sedimentation: Acoustic basement subtracted by Merged_U3a&U3b

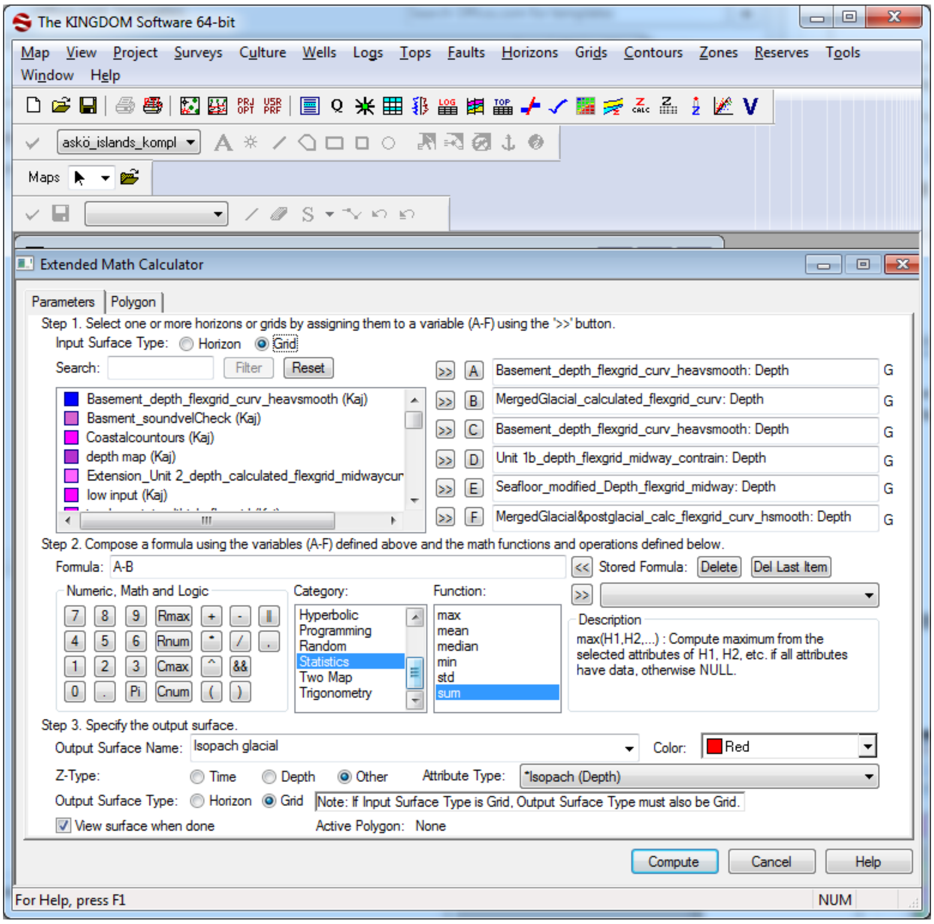

Figure 29: Basement grid subtracted by Glacial grid

Observe that the Z-type is set to Other->Isopach(Depth)

Press compute

2) Select which grids parameters you wish to use (these are the parameters that where defined when the selected grid was built)

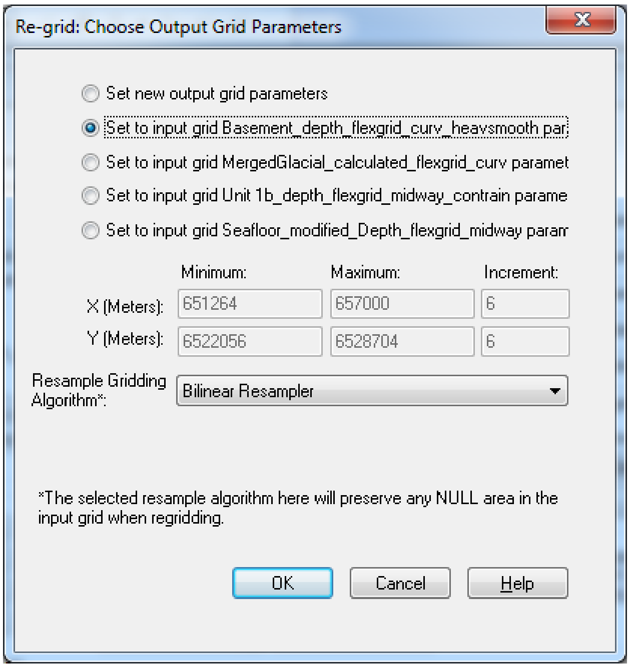

Merging Horizons

Since some subunits for two of the events were defined in this project it was necessary to merge these horizons for the isopach grid calculations.

1) The formula or(A,B) is used to create one horizon which picks the shallowest interpreted points in the two units 3a and 3b

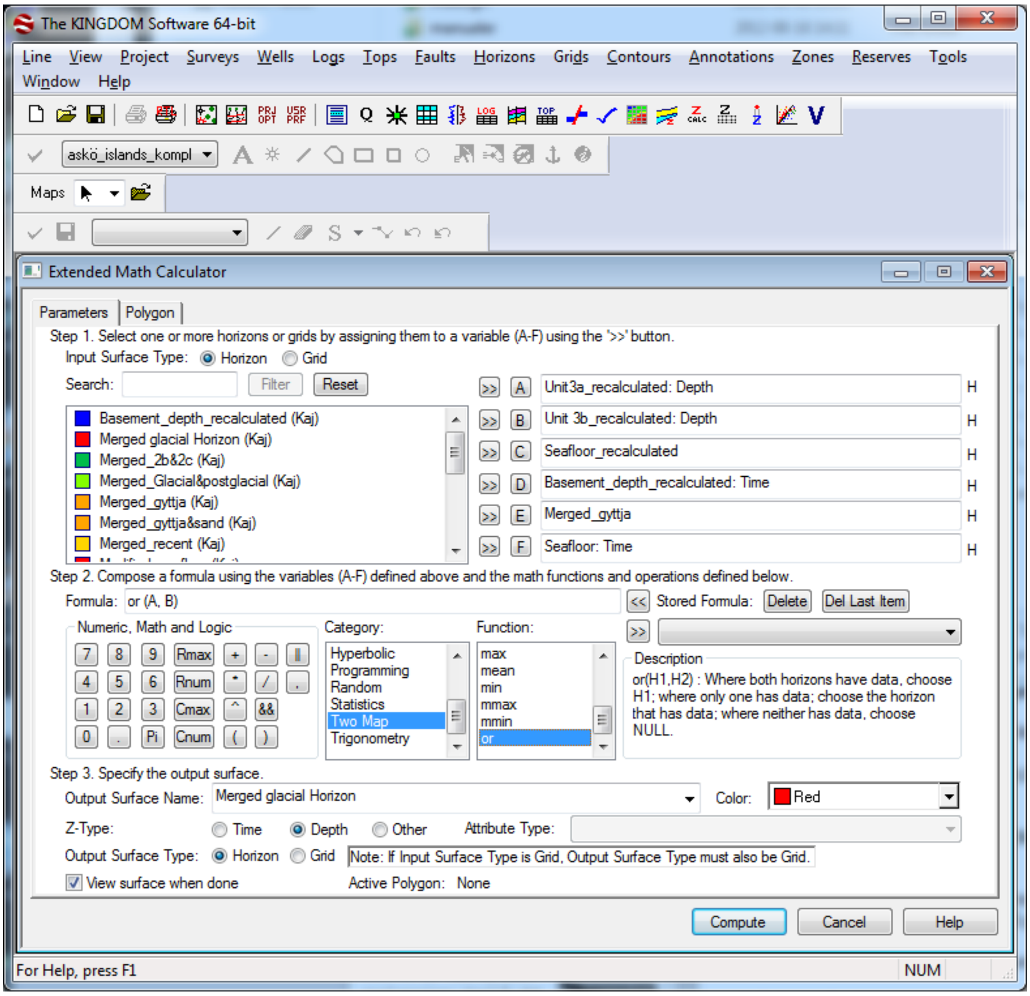

Constraining Grids

To prevent extrapolating in unwanted areas the grid in this project was first constrained by constructing a polygon which were selected in grid parameters as the grids where created.

To further prevent the grid from extrapolating through other interpreted units it was further constrained by using the extended calculator.

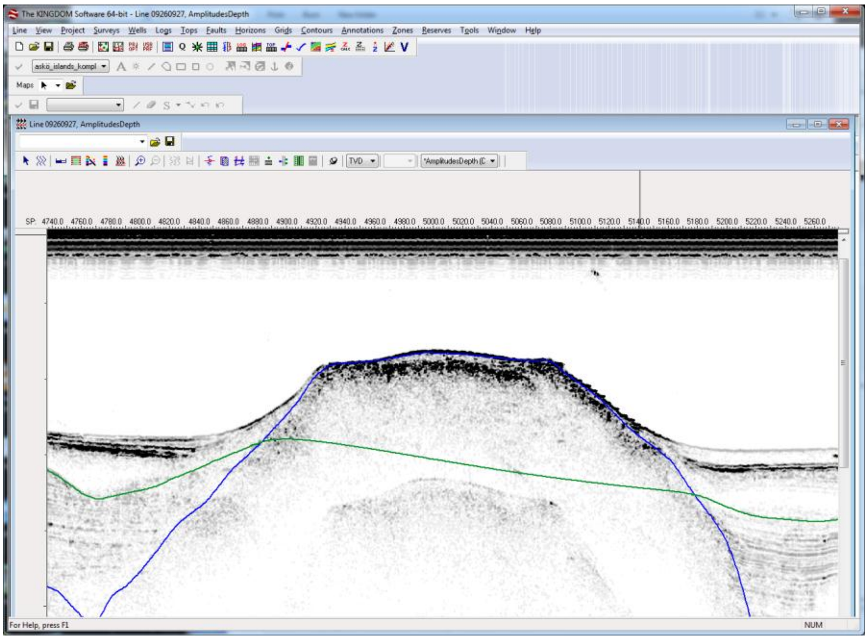

Figure 30: The grid for Merged_U3a_U3b (green) extrapolates through the Gridded Acoustic basement (blue) and so gives a false impression of its extension in the area.

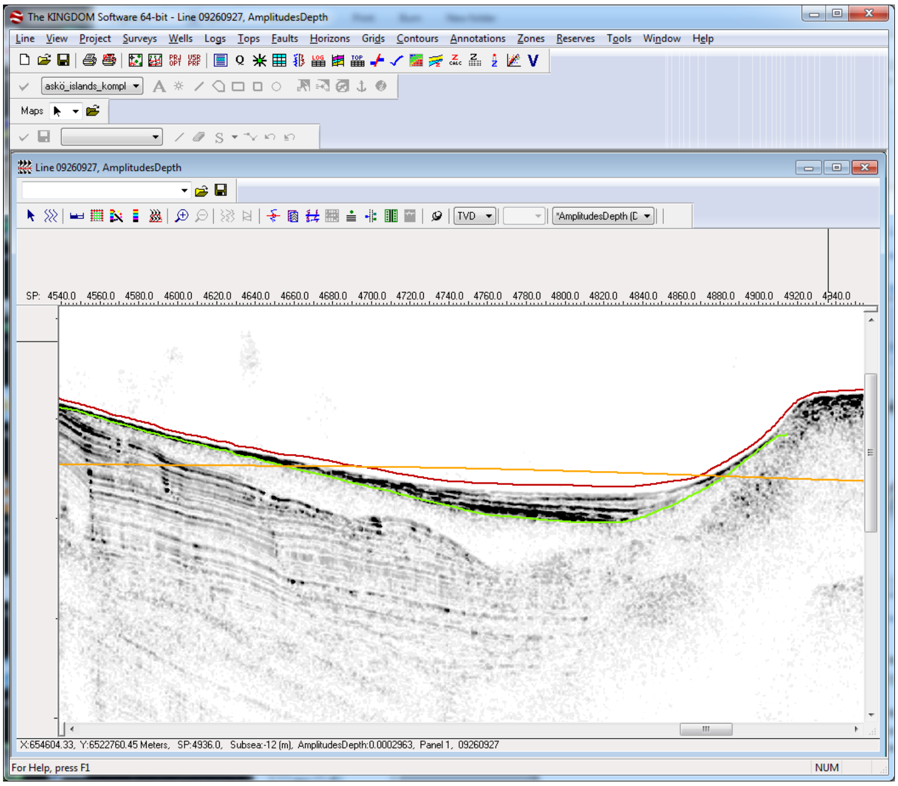

Figure 31: The grid for U1a_Gas (orange) extrapolates through the Merged_U3ab_U2 (Light green) over the Modified seafloor grid (Red).

1) The following formulas were used:
   bmax(H1, H2): (Blanking maximum) Result is NULL if both horizons have data and H1>H2, otherwise H1. Were used to prevent one grid to extrapolate through another grid (fig. 1).
   bmin(H1, H2) : (Blanking minimum) Result is NULL if both horizons have data and H1<H2, other H1. Where used to prevent the grids from extrapolating more than 1m above the

seafloor. Since the top most grid have the same depth as the “True” seafloor grid, i.e. H1=H2, the formula cannot be used. For this a “Modified Seafloor” grid were created using Horizon snap (explained below) to rise the seafloor horizon by 0.5-1m.

Several combinations of the formula bmax() was used depending on which grid that where to be constrained. Generally the rule is; all grids located lower than the grid to be calculated is included in the constraint formula and the bmax() function:

- Recent unit calculation: bmax(**Merged_U1ab_U1c**, **Acoustic basement**)&&bmax(**Merged_U1ab_U1c**, **Merged_U2_U3ab**)&&bmin(**Merged_U1ab_U1c**, **Modified seafloor**)
- Glacial unit calculation: bmax(Merged_U3a_U3b, Acoustic basement)&&bmin(Merged U3a_U3b, Modified seafloor)

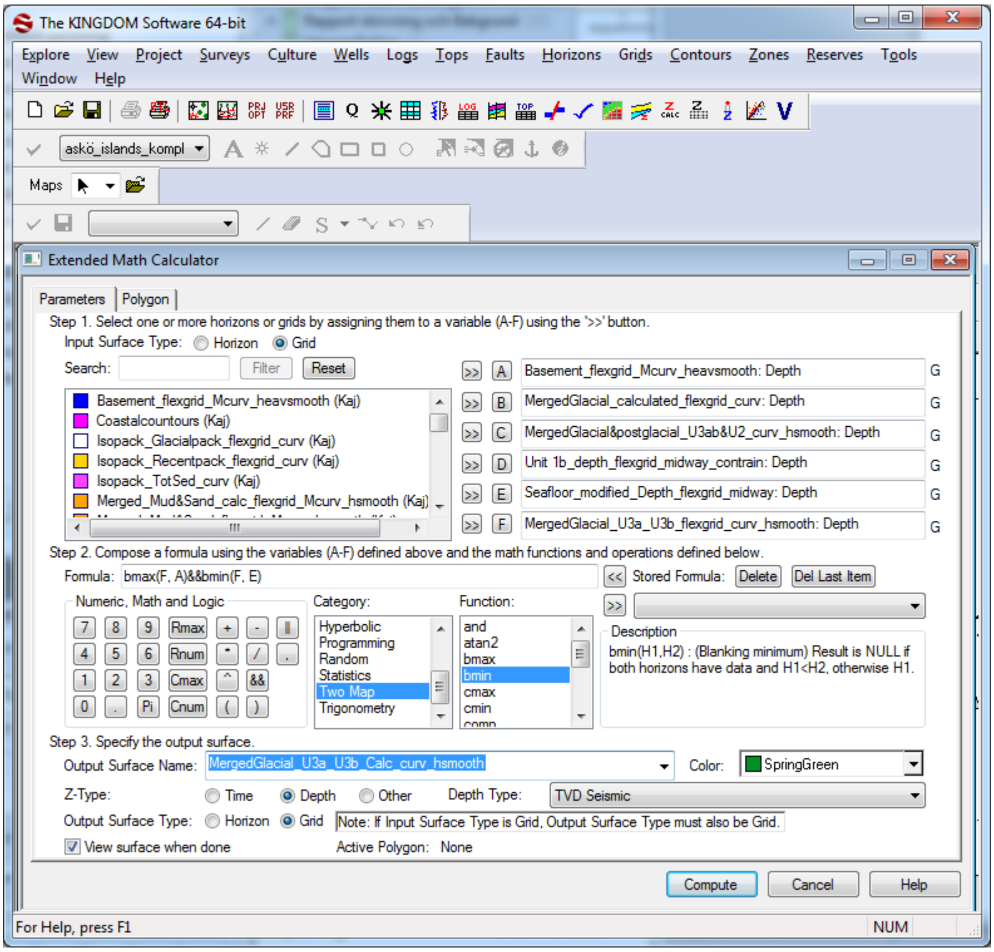

Figure 32: Calculating the Glacial Unit in extended math calculator

2) After the input of the formula Z-type **depth** are chosen and set the **depth type** *TVD seismic* to get positive values or *Subsea* to get negative values . Press compute

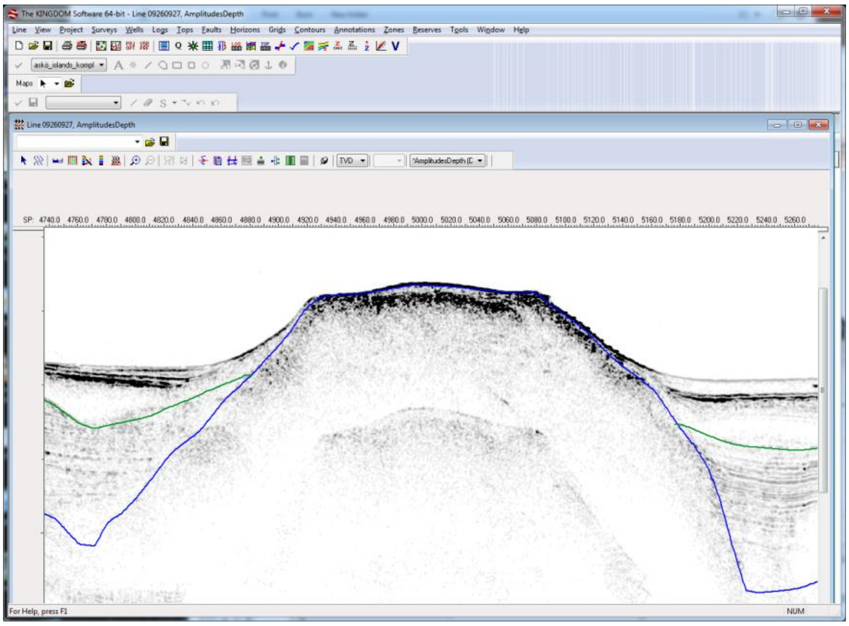

Figure 33: Comparing to Fig. 2 the calculated Merged_U3a_U3b grid (Green) do not extrapolate through the Acoustic basement grid (Blue) any longer

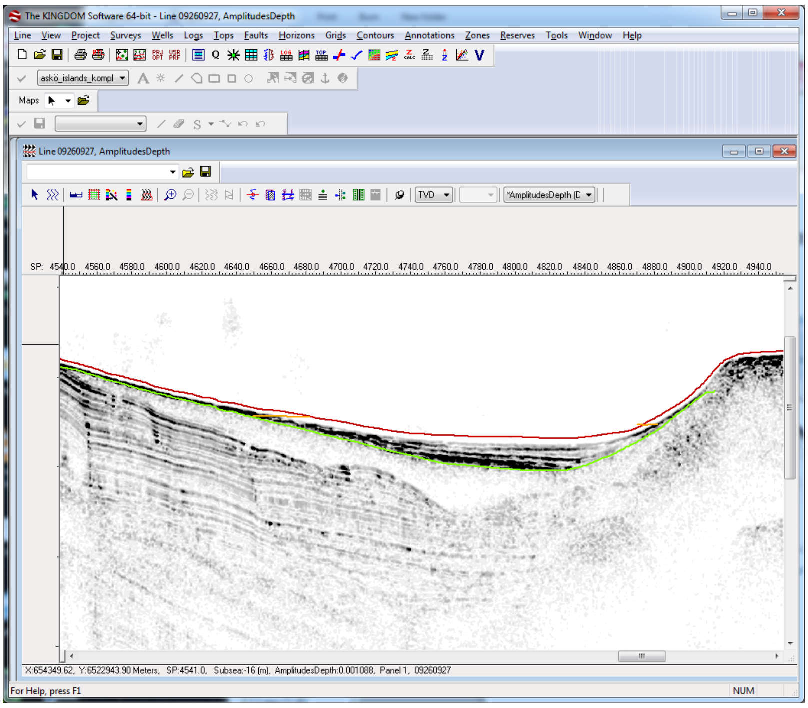

Figure 34: The calculated grid for U1a_Gas (orange) do not longer extrapolates through the Merged_U3ab_U2 (light green) thanks to the bmax() function or over the Modified seafloor grid (Red) thanks to the bmin() function. Small patches still remains though and are edited manually.

Manipulating grids and Horizons

Horizon snap

This is used to lower or raise a group of horizons, for example, in cases when a different sound velocity is applied on datasets with already interpreted horizons.

1) Select the horizon snap tool: Horizons -> horizon snap

2) Choose the horizon to manipulate together with its domain.

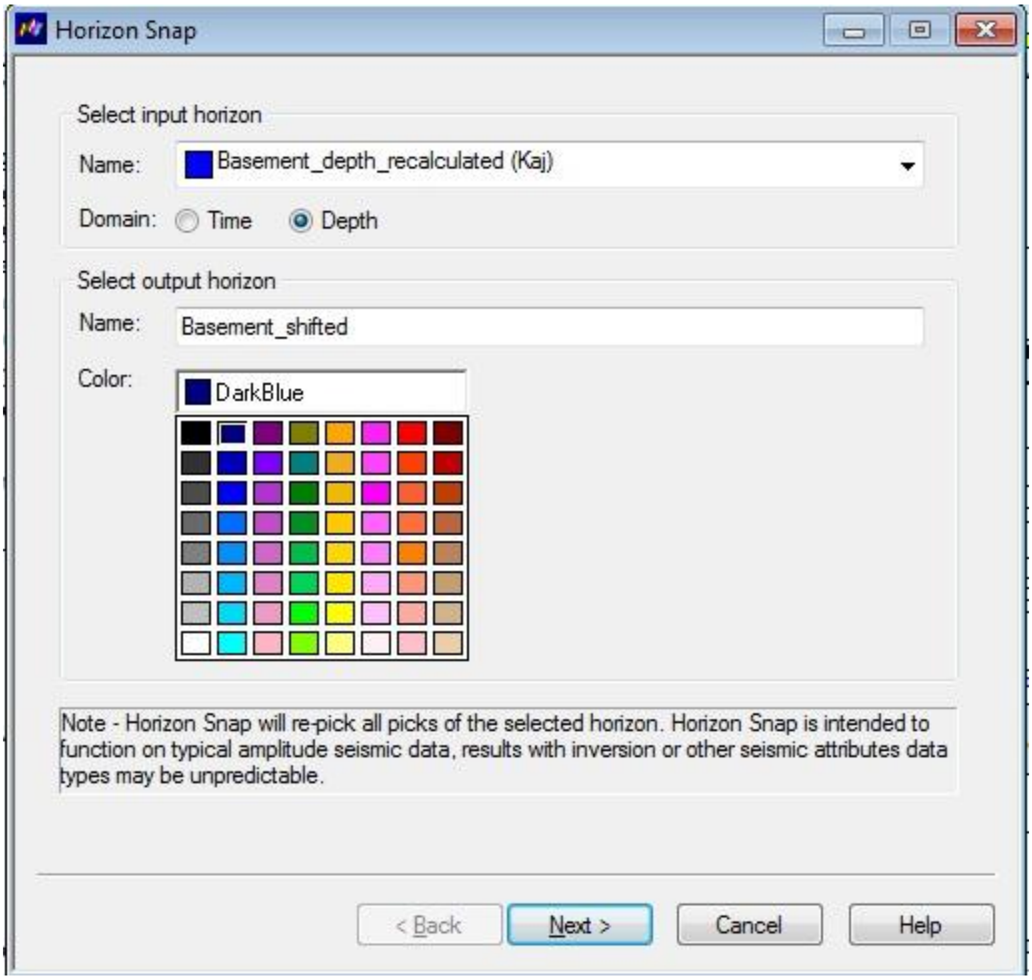

- To manually choose a depth for the guide window chose define guide window.
- Guide window length: 80m, the depth does not exceed this .
- Guide window position: starting at offset pick and extend above- to extend upward.
- Window offset direction : up - will be shifted upward.
- Window offset distance : 1m-to shift the horizon one meter.
- Select a new horizon snap trace event : Relative peak.

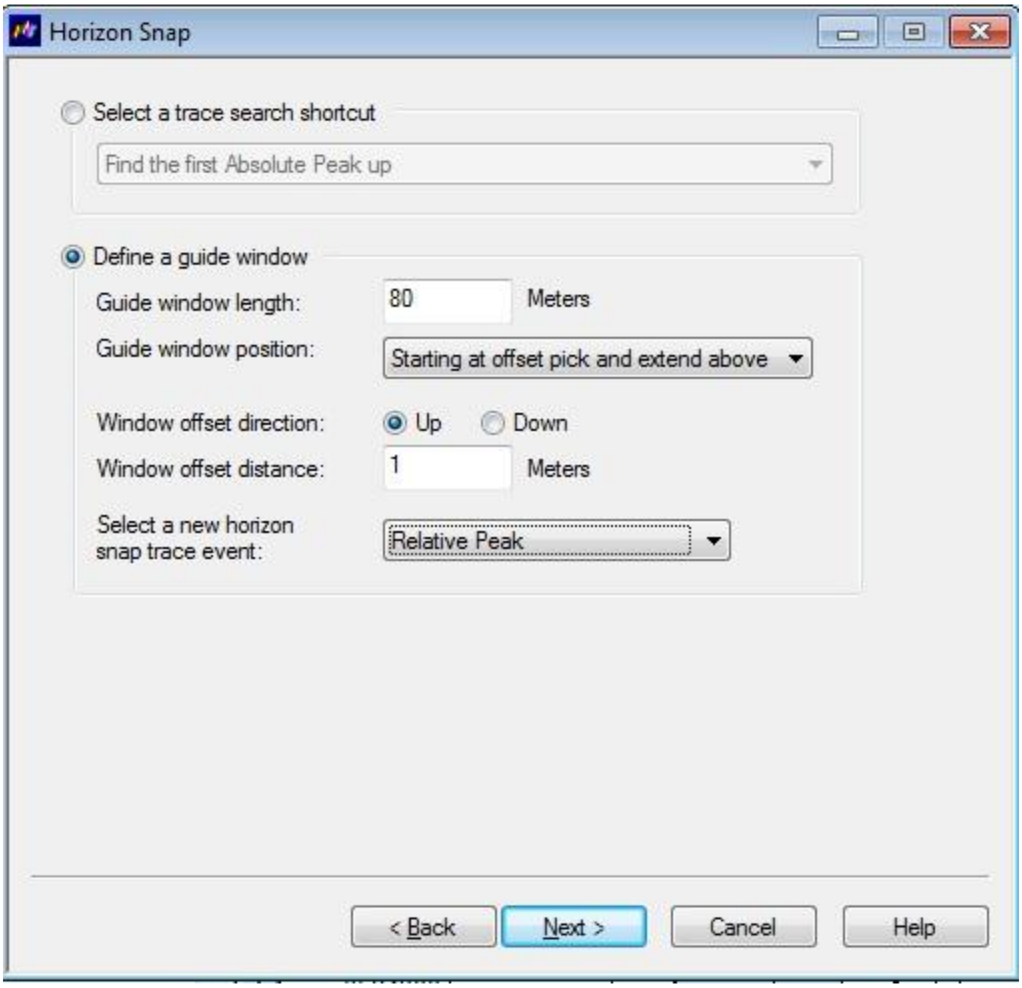

3) Just confirm the steps following.

Grid direct edit

To manually manipulate a grid the direct edit tool can be used.

The tool I accessed under:

➔ Grids -> Direct edit-> shaping tool

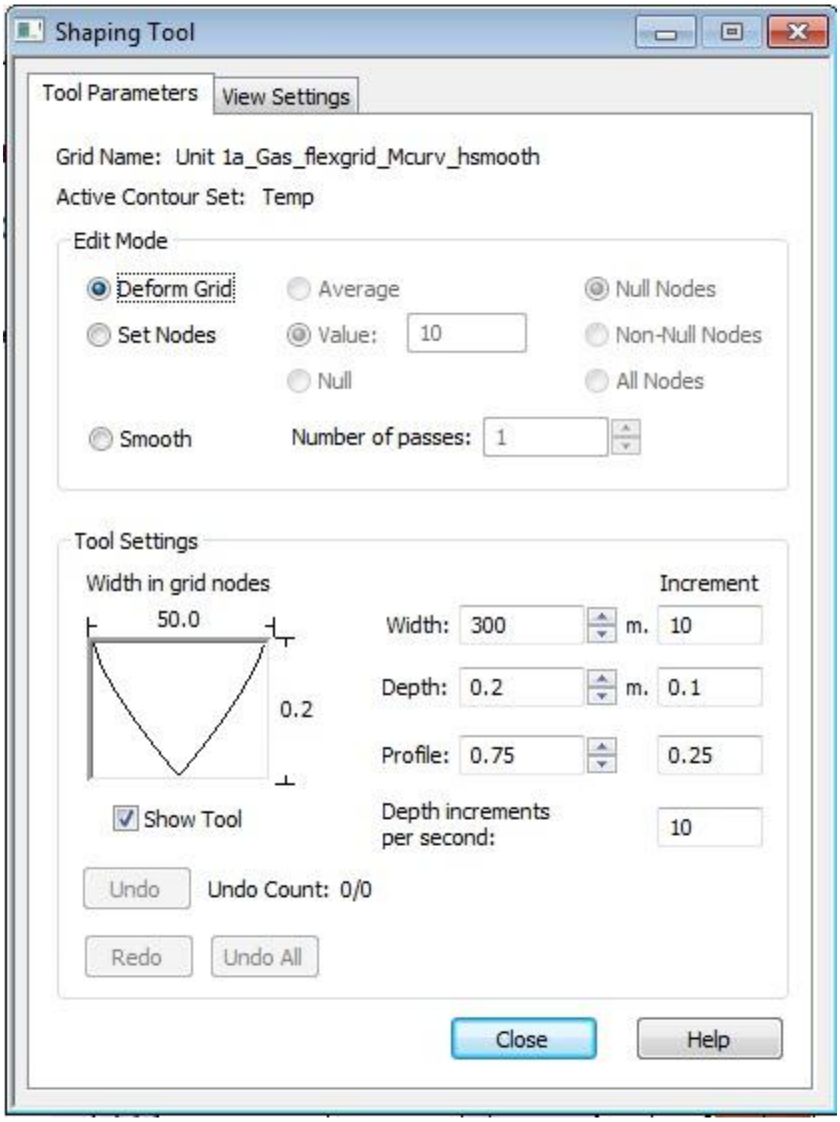
Shaping Tool
Tool Parameters
View Settings
Grid Name: Unit 1a_Gas_flexgrid_Mcurv_hsmooth
Active Contour Set: Temp
Edit Mode
Deform Grid
Average
Null Nodes
Set Nodes
Value: 10
Non-Null Nodes
Null
All Nodes
Smooth
Number of passes: 1
Tool Settings
Width in grid nodes
50.0
0.2
Increment
Width: 300 m. 10
Depth: 0.2 m. 0.1
Profile: 0.75 0.25
Show Tool
Depth increments per second: 10
Undo
Undo Count: 0/0
Redo
Undo All
Close
Help